

Quarterly Report, Volume III

PLANETARY SOLAR ARRAY DEVELOPMENT

Prepared for  
Jet Propulsion Laboratory  
California Institute of Technology  
4800 Oak Grove Drive  
Pasadena, California  
Attention: M. Beckstrom

Contract 952035

EOS Report 7254-Q-3

15 April 1968

Prepared by  
R. Wizenick, Program Manager

Approved by



W. Menetrey, Manager  
Space Electronics Division

This work was performed for the Jet Propulsion  
Laboratory, California Institute of Technology,  
as sponsored by the National Aeronautics and  
Space Administration under Contract No. NAS7-100.



**ELECTRO - OPTICAL SYSTEMS, INC.**

A XEROX COMPANY

PRECEDING PAGE BLANK NOT FILMED.

ABSTRACT

This is the third quarterly report describing the work completed at Electro Optical Systems, Inc. of the Planetary Solar Array Development Study Program, Jet Propulsion Laboratory Contract No. 952035.

This report finalizes the requirements of Task III, and is presented in three volumes.

CONTENTS

1.	INTRODUCTION	1-1
2.	PACKAGING AND DEPLOYMENT	2-1
2.1	Packaging	2-1
2.2	Deployment	2-6
3.	ELECTRIC ANALYSIS	3-1
3.1	Solar Cells	3-1
3.2	Solar Cell Covering	3-1
3.3	Solar Cell Radiation Degradation	3-1
3.4	Circuit Design	3-1
3.5	Electrical Power Analysis	3-7
3.6	Magnetic Field Analysis	3-18
3.6.1	Magnetic Flux Calculation	3-23
3.6.2	Conclusion	3-27
4.	STRUCTURAL DESIGN AND ANALYSIS	4-1
4.1	Substrate	4-1
4.1.1	Description	4-1
4.1.2	Material Selection	4-2
4.1.3	Mathematical Models	4-2
4.1.4	Critical Load Analysis	4-3
4.1.5	Stress Analysis	4-5
4.2	Structure	4-8
4.2.1	Vertical Boom	4-8
4.2.2	Launch Support Truss	4-15
5.	SYSTEM ANALYSIS	5-1
5.1	Environmental Interactions	5-1
5.2	Material Evaluation	5-1
5.3	Thermal Analysis	5-1
5.4	Weight Analysis, Single-Panel-Oriented Array	5-1
5.5	Reliability Considerations for the Two-Axis Vertically Mounted Array	5-1

## CONTENTS (contd)

5.5.1	Physical Description	5-1
5.5.2	Reliability Definition	5-4
5.5.3	Power Capability	5-4
5.5.4	Failure Mode Discussion	5-4
5.5.5	Analysis	5-5
5.5.6	Conclusions	5-8
6.	PRELIMINARY MANUFACTURING PLAN	6-1
7.	PRELIMINARY TEST PLAN	7-1
7.1	Introduction	7-1
7.1.1	Definitions	7-1
7.2	Solar Array Tests	7-2
7.2.1	Engineering Evaluation Test	7-2
7.2.2	Prototype Testing	7-4
7.2.3	Acceptance Test	7-5
7.2.4	Qualification Test	7-6
7.2.5	Formal Type Approval Test	7-6
7.2.6	Reliability Test	7-9
7.2.7	Shipping Container Test	7-10
7.3	Test Equipment and Fixtures	7-10
7.4	Performance Testing	7-11
7.4.1	Single Cell Testing	7-11
7.4.2	Submodule Testing	7-11
7.4.3	Sample Module Testing	7-11
7.4.4	Panel Testing	7-12
8.	SUMMARY	8-1

## SECTION 1

### INTRODUCTION

This report is Volume III of three volumes of the third quarterly report. It represents the detailed study of the single-panel-oriented solar array.

To avoid repetition, certain sections of this report are referenced to Volume I and II as applicable.

## SECTION 2

### PACKAGING AND DEPLOYMENT

This section details the mechanical packaging and deployment of a photovoltaic power system having sun tracking capability. The system consists basically of a four-section solar panel which is mounted universally on a vertically standing boom. The deployment and positioning mechanisms of the main antenna system are integrated with and driven through this same vertical boom assembly.

This four-section-oriented solar array and integrated antenna system, as well as support and deployment elements, are depicted on Electro-Optical Systems Drawing Number 7254-117 (Fig. 2-1). Included is a legend for identification of the various mechanical and structural elements of the system. Reference is also made to Electro-Optical Systems Drawing Number 7254-119 which appears in Section 3 of this text (Fig. 3-13) and which depicts enlarged views of the four-section solar array with its structural and deployment elements. This design provides for the solar panels being mounted in such a manner that three sides of the spacecraft are always completely unobstructed. It overcomes the possibility of the antenna output being blocked by the solar array, or the solar array being shadowed by the antenna.

#### 2.1 PACKAGING

The following is a discussion of the mechanical aspects for a conceptual design of a photovoltaic power system which meets the design constraints of Jet Propulsion Laboratory Drawing No. 1002-3236A, and Electro-Optical Systems Drawing No. 7254-100 (Fig. 2-2, Volume II). The design provides for solar cell circuits being permanently affixed to one side only of

16

15

14

13

SECURITY CLASSIFICATION

I  
H

NOTES: UNLESS OTHERWISE SPECIFIED

G

F

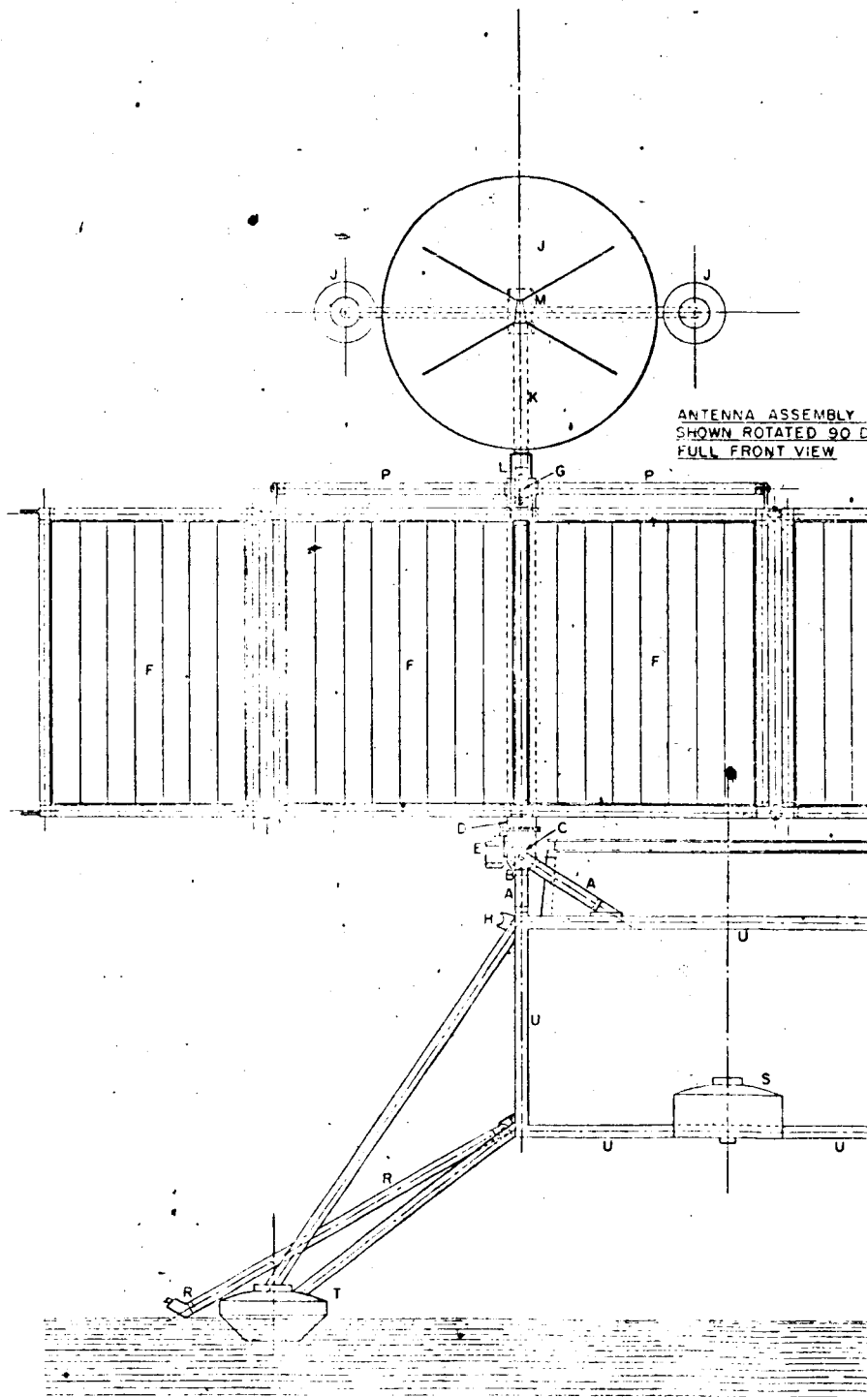
E

D

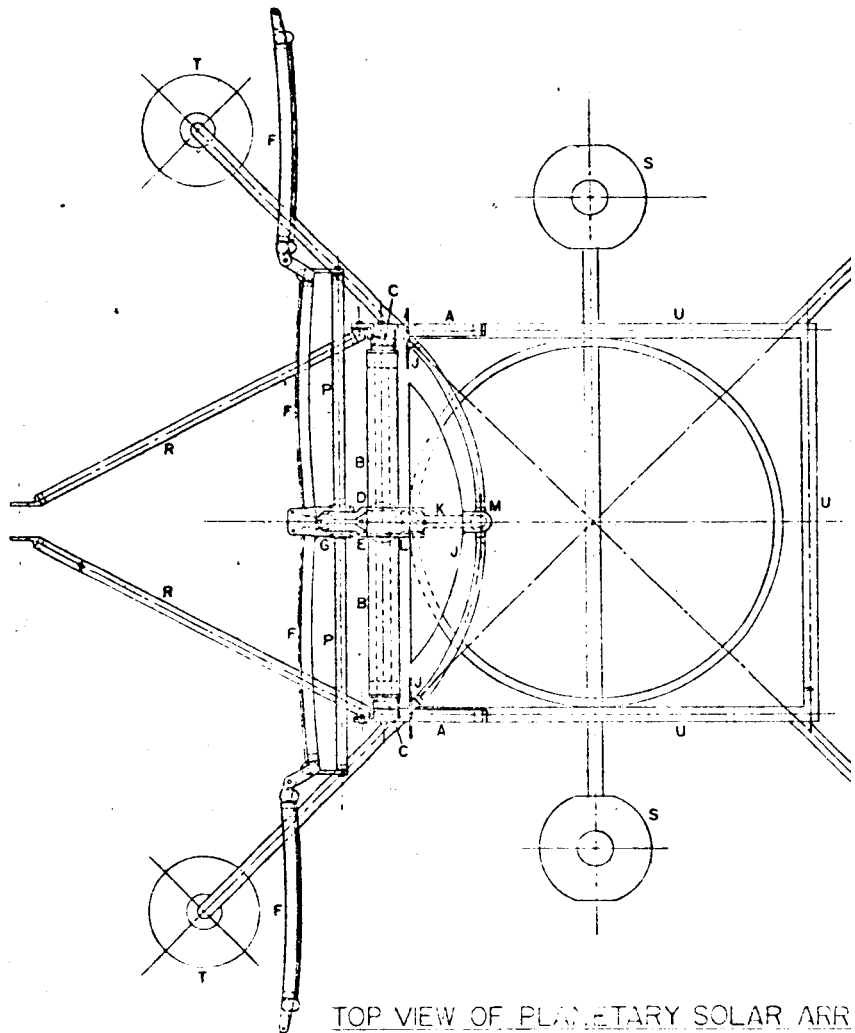
C

B

A

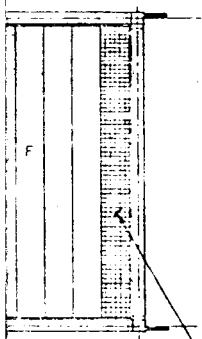


ANTENNA ASSEMBLY  
SHOWN ROTATED 90 D  
FULL FRONT VIEW



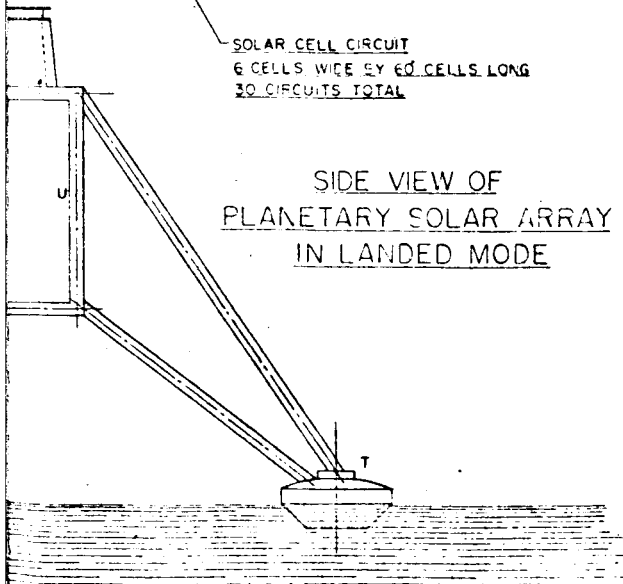
TOP VIEW OF PLANETARY SOLAR ARR  
IN LANDED AND DEPLOYED CONDITION

AND SOLAR ARRAY  
FIGURES TO SHOW



SOLAR CELL CIRCUIT  
6 CELLS WIDE BY 40 CELLS LONG  
30 CIRCUITS TOTAL

SIDE VIEW OF  
PLANETARY SOLAR ARRAY  
IN LANDED MODE

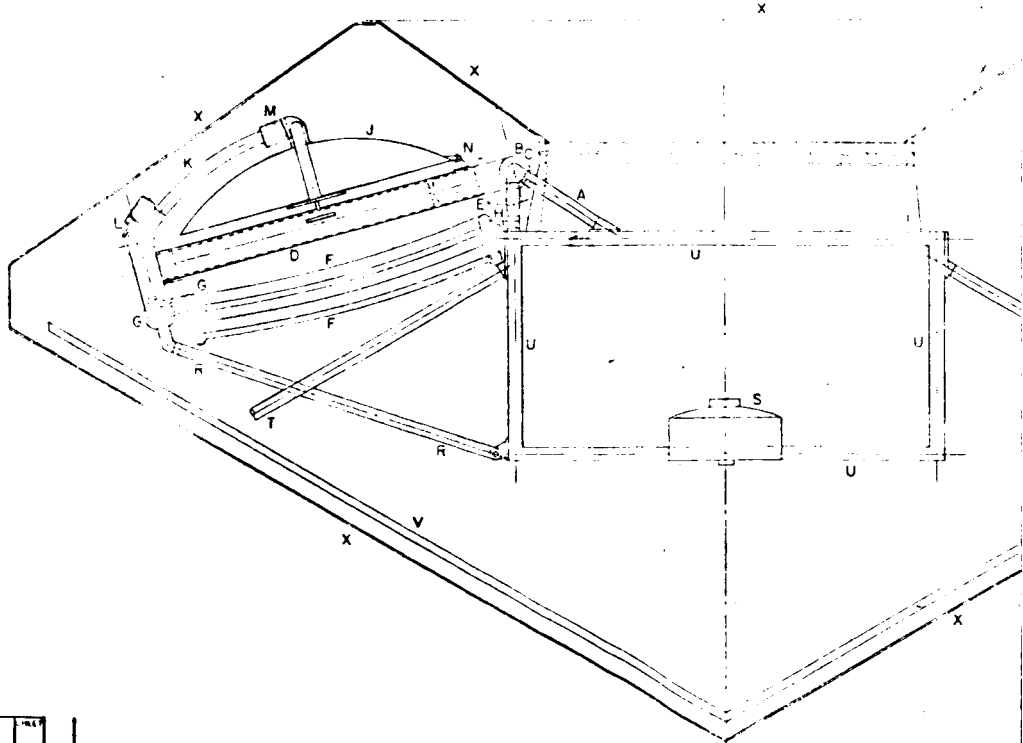




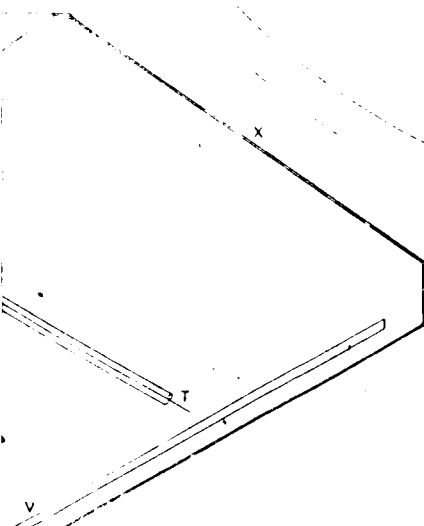
## LEGEND

- A - MAIN SUPPORT BRACKET ASSEMBLY
- B - BOOM PIVOT SHAFT
- C - BOOM ELEVATING TENSION SPRING AND LOCK MECHANISM
- D - VERTICAL BOOM ASSEMBLY
- E - BOOM ROTATING DRIVE MECHANISM
- F - SOLAR PANEL ASSEMBLY
- G - SOLAR PANEL ASSEMBLY ELEVATION DRIVE MECHANISM
- H - SOLAR PANEL ASSEMBLY LAUNCH MODE LATCH
- J - ANTENNA ASSEMBLY
- K - ANTENNA BOOM
- L - ANTENNA ELEVATION DRIVE MECHANISM
- M - ANTENNA ROTATION DRIVE MECHANISM
- N - ANTENNA LAUNCH MODE LATCH
- P - SOLAR PANEL HINGE PIVOT SHAFT
- R - LAUNCH MODE SUPPORT TRUSS
- S - LANDING RADAR
- T - LANDING FOOT
- U - SPACECRAFT BODY
- V - HEAT SHIELD
- X - STERILIZATION CANNISTER

NOTE: FOR ENLARGED VIEW OF SOLAR PANEL, SHOWING FRAME AND  
DEPLOYMENT MECHANISM, SEE SOLAR PANEL ASSEMBLY,  
E O S DRAWING NUMBER J 7254-119.



H
G
F
E
D
C
B



SIDE VIEW OF PLANETARY SOLAR ARRAY  
IN STOWED OR LAUNCH CONDITION

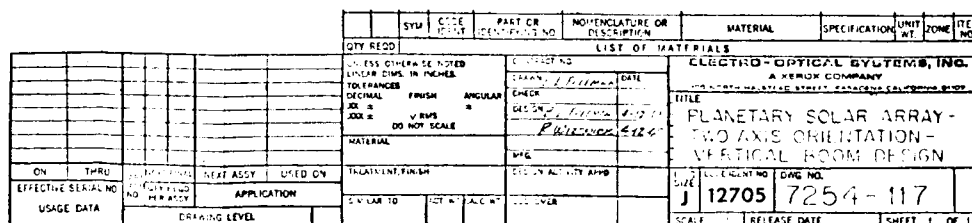
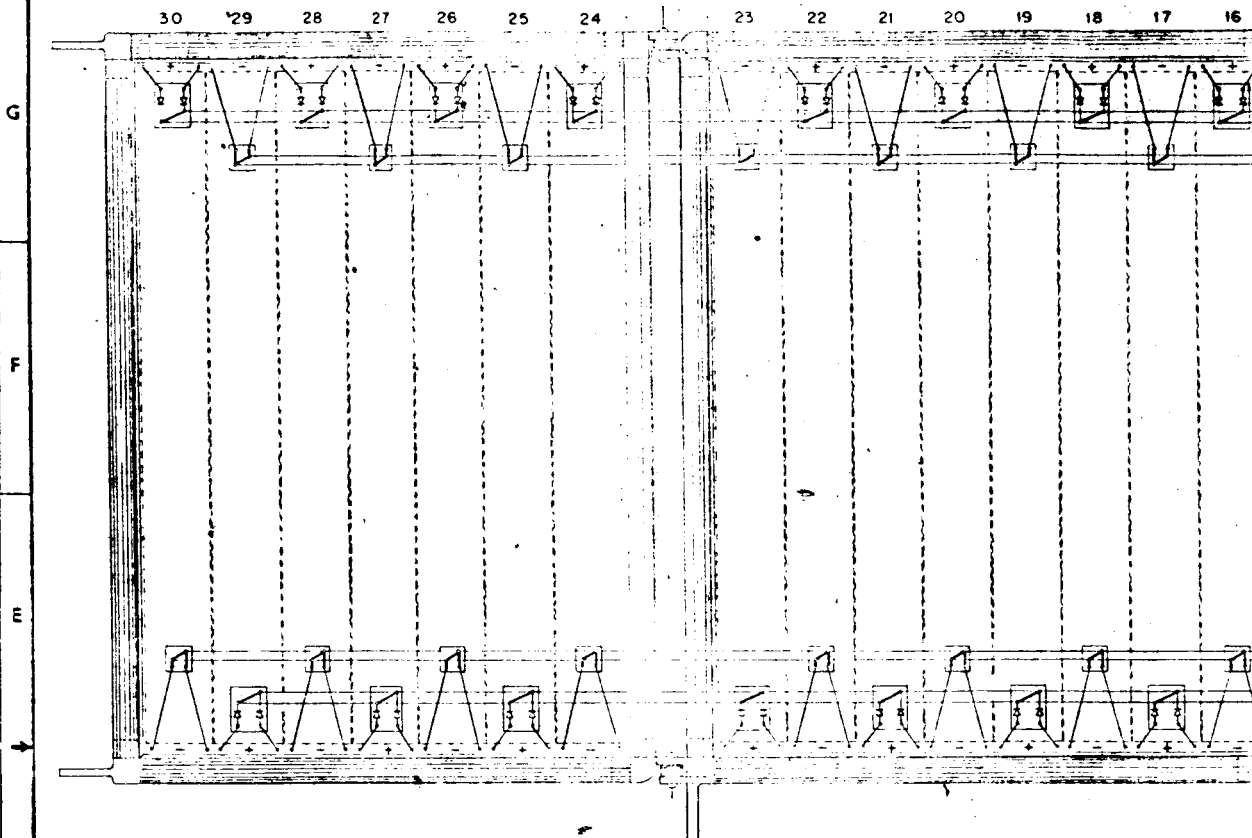
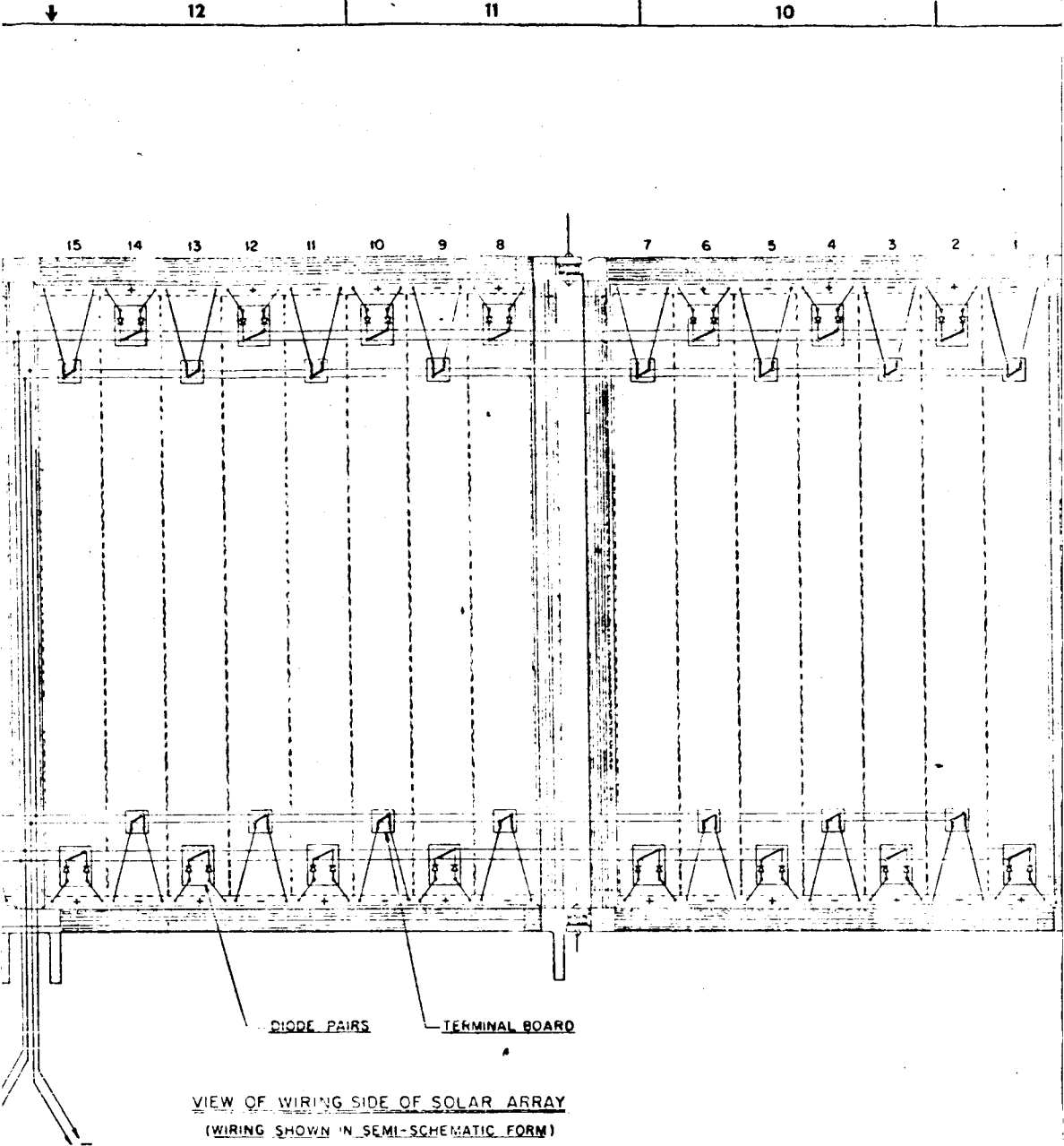


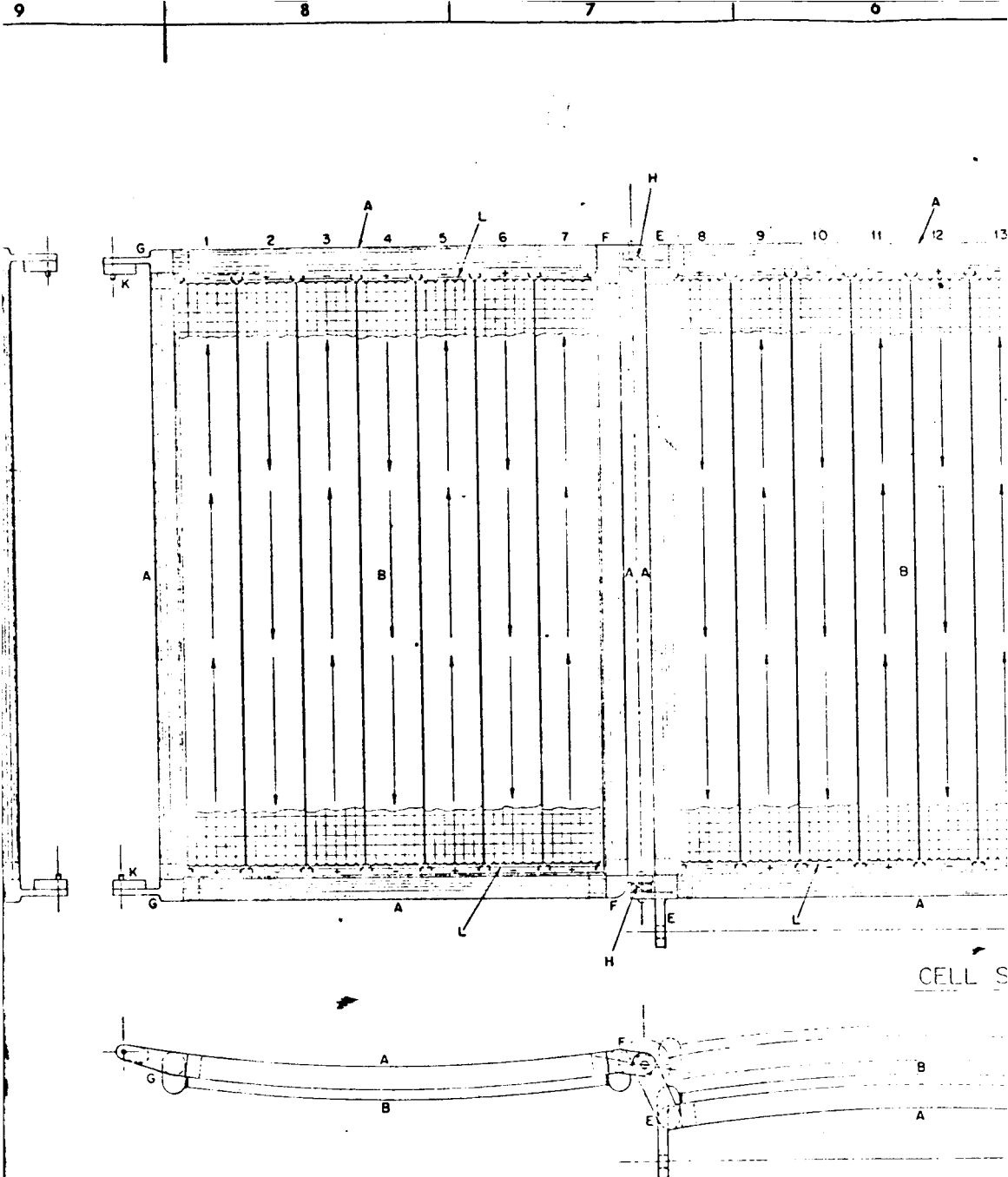
Figure 2-1. **Fold out**  
**FRAME 4**

H

NOTES: UNLESS OTHERWISE SPECIFIED







# LEGEND

- A - BERYLLIUM TUBING FRAME
- B - HOLLOWCORE SUBSTRATE
- C - CENTER PIVOT HINGE AND LATCH FITTING
- D - CENTER LATCH FITTING
- E - END HINGE AND LATCH FITTING
- F - END HINGE FITTING
- G - END LATCH FITTING
- H - TORSION SPRING PANEL DEPLOYMENT MECHANISM
- K - LATCH MECHANISM
- L - ELECTRICAL CIRCUIT END TERMINATION

1A

PRECEDING PAGE BLANK NOT FILMED.

the substrate of each of four major segments or panels of which the complete photovoltaic array is composed. Each segment or panel is in the form of an aluminum, hollow-core substrate with integral beryllium tubing frames around its periphery. Special miniature aluminum extrusions are used as the bridge element from the hollow-core substrate to the beryllium tubing frames. The two center segments are bonded together in such a manner that they form a single, rigid assembly of sufficient area to contain 16 solar circuits (eight circuits on each segment or panel). On this portion of the solar array, the cells are bonded onto the convex surface of the panels.

The two outer segments or panels are hinged to the frame of the center double panel, one on each end, in such a way that they can be folded inward toward the boom assembly, D, and securely latched during the stowed or launch condition. Each of the two end panels is of sufficient area to contain seven solar circuits which are bonded to the concave surface of the substrate, thereby affording greater packaging density when the panels are in the folded and latched condition. The total solar array, F, contains 30 solar circuits, each of which contains six cells in parallel by 60 cells in series.

During the launch condition, the folded solar array will be mounted within the sterilization cannister on an angle of 15 degrees below horizontal. In this condition, it is centrally located beneath the main boom assembly, D. The side of the array, which is not attached to the outboard end of the boom, is folded in against, and latched onto, the upper frame of the spacecraft body, U.

The outboard end of the boom assembly is supported in the stowed condition by the two thin-wall beryllium tubes with lightweight metal end fittings. These tubes are positioned to form an "A frame" truss, R, which terminates at each side of the bottom of the spacecraft frame.

The antenna assembly, J, is mounted by means of its own antenna boom, K, and a latch mechanism, N, directly above the main boom assembly.

The inboard end of the main boom assembly is attached to the top of the spacecraft through the boom pivot shaft, B, to a main support bracket assembly, A, which is located at each side of the top of the spacecraft frame. The two main support bracket assemblies, boom pivot shaft, and main boom assembly are composed of thin-wall beryllium tubing with lightweight metal end fittings. Various torsion spring assemblies, latch and unlatch units, and drive motors are used for positioning the solar array and antenna assembly in the landed condition, and will be described in the following paragraphs.

## 2.2 DEPLOYMENT

Upon landing, deployment and positioning of the solar array and antenna assembly will be accomplished in a sequential manner by a preprogrammed routine from the spacecraft computer. First, the two a frame truss members will be unlatched and released from the outboard end of the main boom assembly. This will allow these truss members to fall down to the surface of the terrain upon which the spacecraft has landed. Second, the solar array latches, H, will be released, which will completely unlock the integrated system from the stowed or launch condition. Unlatching will be accomplished pyrotechnically.

After unlatching, two torsion spring mechanisms, C, which are located at each end of the boom pivot shaft, will lift the entire integrated system and rotate it in an upward direction through 105 degrees to a vertical position parallel to the vertical centerline of the spacecraft. The torsion spring mechanisms are equipped with damper devices and locks which will slow the movement of the system as it approaches the end of its travel, and lock it into a rigid condition when it reaches the vertical position.



After the boom has been elevated and locked in the vertical position, the latches which have been holding the two outer solar panels in the stowed condition will be unlatched pyrotechnically. Torsion spring mechanisms located at each outer panel hinge fitting will rotate the two outer solar panels through 180 degrees outward from their folded, or stowed, position. The torsion spring mechanisms are equipped with damper devices and locks which will slow the outward movement of the panels as they approach the end of their travel, and lock them into a full extended position as shown in the drawing.

The entire vertical boom assembly, which carries the solar array and the antenna assembly, is free to rotate a full 360 degrees about its axis. This rotation is accomplished by means of the boom rotating drive mechanism, E, which is located at the base of the vertical boom and which is basically a completely enclosed and dustproof gear motor. Elevation or tilt of the solar array is accomplished by means of the solar panel assembly elevation drive mechanism, G, which is located at the junction point of the solar array and the outboard end of the vertical boom assembly. This mechanism is basically a second completely enclosed and dustproof gear motor, the purpose of which is to elevate the solar array, as required. By movement of these two drive mechanisms, any desired angular position or elevation of the solar array can be achieved.

Initial positioning of the planetary solar array will be accomplished from preprogrammed commands which have been stored in the spacecraft computer and logic system, or from earth command. This involves rotating and elevating the array so that it "finds" the sun. After proper initial positioning, the solar array will "lock onto the sun" by means of solar sensing device which is located at the end of the array, it will continue to track the sun throughout the Martian day. At the end of each Martian day, the solar array will be returned to the "sunrise condition" by either the spacecraft computer or earth command. The

rotating boom will be programmed to always return to the "sunrise condition" by reversing its direction of rotation. Slip rings on the boom for power transmission will therefore not be necessary, and power and control leads can be brought out to the spacecraft through the hollow boom.

The main antenna assembly, J, is integrated with, but operates independently with respect to, the vertical boom assembly, D. After the spacecraft has landed and the boom assembly has been elevated and locked in its vertical position, the antenna assembly will be unlatched pyrotechnically from its stowed or launch condition. It is then free to be elevated as required by the antenna elevation drive mechanism, L, located on top of the vertical boom assembly. Full 360 degree angular rotation of the antenna assembly is achieved by means of the antenna rotation drive mechanism, M. These two drive mechanisms are basically completely enclosed and dustproof gear motors. By the independent operation of each motor, the antenna assembly can be aimed in any desired direction. Antenna assembly positioning will be achieved by command from either the spacecraft computer or from earth command.

## SECTION 3

### ELECTRIC ANALYSIS

This section details the electrical analysis for the single-panel-oriented solar array.

- |   |   |           |
|---|---|-----------|
| 3.1 <u>SOLAR CELLS</u>                      | } | REFERENCE |
| 3.2 <u>SOLAR CELL COVERING</u>              |   |           |
| 3.3 <u>SOLAR CELL RADIATION DEGRADATION</u> |   | VOLUME II |
| 3.4 <u>CIRCUIT DESIGN</u>                   |   |           |

The electrical circuit shall be a flat-mounted array of series-parallel solar cells of 6P x 60S. The dimensions of the circuit are shown in Fig. 3-10, drawing 7254-120. The electrical connector configurations are shown in Figs. 3-11 and 3-12. The reasons for preferring this type of circuit configuration were discussed in the second quarterly report.

A drawing of the panel is shown in EOS drawing 7254-119, Fig. 3-13. The panel array is considered as a single panel; however, in reality it consists of four subpanels. The center section consists of two spherical, hollowcore substrates sharing a common beryllium beam. Each substrate contains 8 circuits of 6P x 60S for a total of 16 circuits. The folding side panels are spherical, hollowcore substrates with beryllium edge beams. They contain 7 circuits each of 6P x 60S. The total number of circuits in the array is 30. The circuits are attenuated in direction to minimize the magnetic field effect, and no

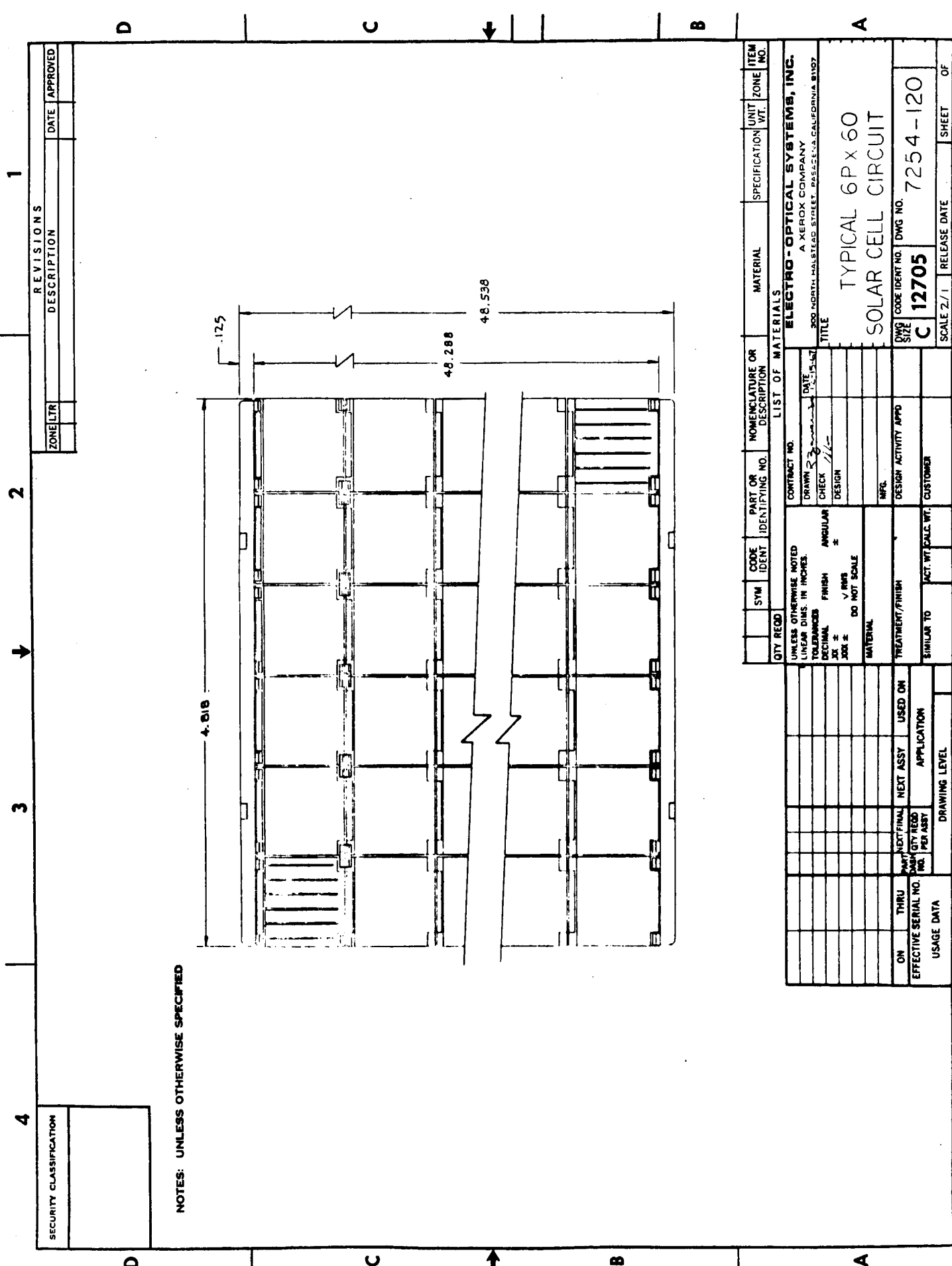


Figure 3-10. Typical 6P x 66 Solar Cell Circuit

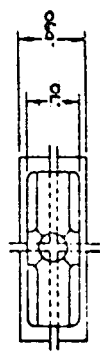
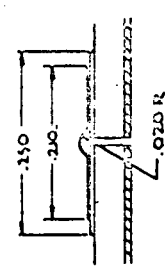
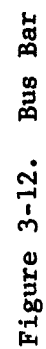
4	3	2	1																											
<div style="display: flex; justify-content: space-between;"> <div style="width: 15%;"> <p>SECURITY CLASSIFICATION</p> </div> <div style="width: 60%;"> <p>REVISIONS</p> <table border="1" style="width:100%; border-collapse: collapse;"> <tr> <th>REV.</th> <th>DESCRIPTION</th> <th>DATE</th> <th>APPROVED</th> </tr> <tr> <td> </td> <td> </td> <td> </td> <td> </td> </tr> </table> </div> <div style="width: 15%;"> <p>ZONE/CTR</p> </div> </div>				REV.	DESCRIPTION	DATE	APPROVED																							
REV.	DESCRIPTION	DATE	APPROVED																											
<div style="display: flex; justify-content: space-around; align-items: center;"> <div style="width: 45%;"> <p>NOTES: UNLESS OTHERWISE SPECIFIED</p>  </div> <div style="width: 45%;">  </div> </div>																														
<table border="1" style="width:100%; border-collapse: collapse;"> <tr> <th>SYN</th> <th>CODE</th> <th>IDENT</th> <th>PART OR IDENTIFYING NO.</th> <th>NOMENCLATURE OR DESCRIPTION</th> <th>MATERIAL</th> <th>SPECIFICATION</th> <th>UNIT</th> <th>ITEM NO.</th> </tr> <tr> <td colspan="9"> <p>QTY REQD</p> <p>UNLESS OTHERWISE NOTED UNLESS DIMS IN INCHES</p> <p>TOLERANCES: DECIMAL FRACTION ANGULAR</p> <p>XX ± .005</p> <p>XXX ± .010</p> <p>DO NOT SCALE</p> <p>NATURAL</p> <p>TREATMENT: FINISH</p> <p>SIMILAR TO</p> <p>ACT. WT. GMS. WT. CUSTOMER</p> <p>WTC</p> <p>DESIGN ACTIVITY APTD</p> <p>DATE</p> <p>CONTRACT NO.</p> <p>DRAWN BY</p> <p>CHECK</p> <p>DESIGN</p> <p>DATE</p> </td> </tr> <tr> <td colspan="9"> <p>LIST OF MAT'L P.C.</p> <p>ELECTRO-OPTICAL SYSTEMS, INC.</p> <p>A XEROX COMPANY</p> <p>7254-Q-3</p> <p>TOP CONTACT TYPE CONNECTOR</p> <p>SIZE C 12705</p> <p>QNS NO. 7254-106</p> <p>SCALE 1/2" = 1" RELEASE DATE</p> </td> </tr> </table>				SYN	CODE	IDENT	PART OR IDENTIFYING NO.	NOMENCLATURE OR DESCRIPTION	MATERIAL	SPECIFICATION	UNIT	ITEM NO.	<p>QTY REQD</p> <p>UNLESS OTHERWISE NOTED UNLESS DIMS IN INCHES</p> <p>TOLERANCES: DECIMAL FRACTION ANGULAR</p> <p>XX ± .005</p> <p>XXX ± .010</p> <p>DO NOT SCALE</p> <p>NATURAL</p> <p>TREATMENT: FINISH</p> <p>SIMILAR TO</p> <p>ACT. WT. GMS. WT. CUSTOMER</p> <p>WTC</p> <p>DESIGN ACTIVITY APTD</p> <p>DATE</p> <p>CONTRACT NO.</p> <p>DRAWN BY</p> <p>CHECK</p> <p>DESIGN</p> <p>DATE</p>									<p>LIST OF MAT'L P.C.</p> <p>ELECTRO-OPTICAL SYSTEMS, INC.</p> <p>A XEROX COMPANY</p> <p>7254-Q-3</p> <p>TOP CONTACT TYPE CONNECTOR</p> <p>SIZE C 12705</p> <p>QNS NO. 7254-106</p> <p>SCALE 1/2" = 1" RELEASE DATE</p>								
SYN	CODE	IDENT	PART OR IDENTIFYING NO.	NOMENCLATURE OR DESCRIPTION	MATERIAL	SPECIFICATION	UNIT	ITEM NO.																						
<p>QTY REQD</p> <p>UNLESS OTHERWISE NOTED UNLESS DIMS IN INCHES</p> <p>TOLERANCES: DECIMAL FRACTION ANGULAR</p> <p>XX ± .005</p> <p>XXX ± .010</p> <p>DO NOT SCALE</p> <p>NATURAL</p> <p>TREATMENT: FINISH</p> <p>SIMILAR TO</p> <p>ACT. WT. GMS. WT. CUSTOMER</p> <p>WTC</p> <p>DESIGN ACTIVITY APTD</p> <p>DATE</p> <p>CONTRACT NO.</p> <p>DRAWN BY</p> <p>CHECK</p> <p>DESIGN</p> <p>DATE</p>																														
<p>LIST OF MAT'L P.C.</p> <p>ELECTRO-OPTICAL SYSTEMS, INC.</p> <p>A XEROX COMPANY</p> <p>7254-Q-3</p> <p>TOP CONTACT TYPE CONNECTOR</p> <p>SIZE C 12705</p> <p>QNS NO. 7254-106</p> <p>SCALE 1/2" = 1" RELEASE DATE</p>																														

Figure 3-11. Top Contact Type Connector



magnetic components are used in the circuits. Each circuit is wired to a terminal board on the back side of the panel with two stranded wire leads for redundancy. Two isolation diodes are placed on the positive terminal board for each circuit, in series with the output leads. The circuits are wired in parallel, with twisted stranded wire, to an outlet plug for the total array.

### 3.5 ELECTRICAL POWER ANALYSIS

The preferred circuit was detailed in the second quarterly report as being 6P x 66S. A closer look at the I-V characteristics of a 1-3 ohm-cm cell revealed that the operating point could be taken as 0.485V instead of 0.450V as originally assumed. An estimate of the temperature of the oriented array for noon sun conditions revealed that the average array temperature would be 28°C, near ambient.

A typical I-V curve of a cell at 28°C is shown in Fig. 3-2, Vol. II.

A new string length of 60 cells in series was selected. The operating point of the cell would be 28.0V plus 1 volt for diode and wiring losses:

$$29.0\text{V}/60 = 483 \text{ mV/cell}$$

As discussed in the second quarterly report, the shift in voltage due to the intensity change from 140 mW/cm<sup>2</sup> to 50 mW/cm<sup>2</sup> is 8 mV (Fig. 3-14). Therefore, referring to Fig. 3-12, of a typical cell at 28°C the current output at 483 mV plus 8 mV (the 8 mV is added instead of subtracted to simulate shifting the curve) is 491 mV, which represents a current of 119.2 mA.

The submodule output would be

$$6 (119.2 \text{ mA}) = 715.2 \text{ mA at } 483 \text{ mV}$$

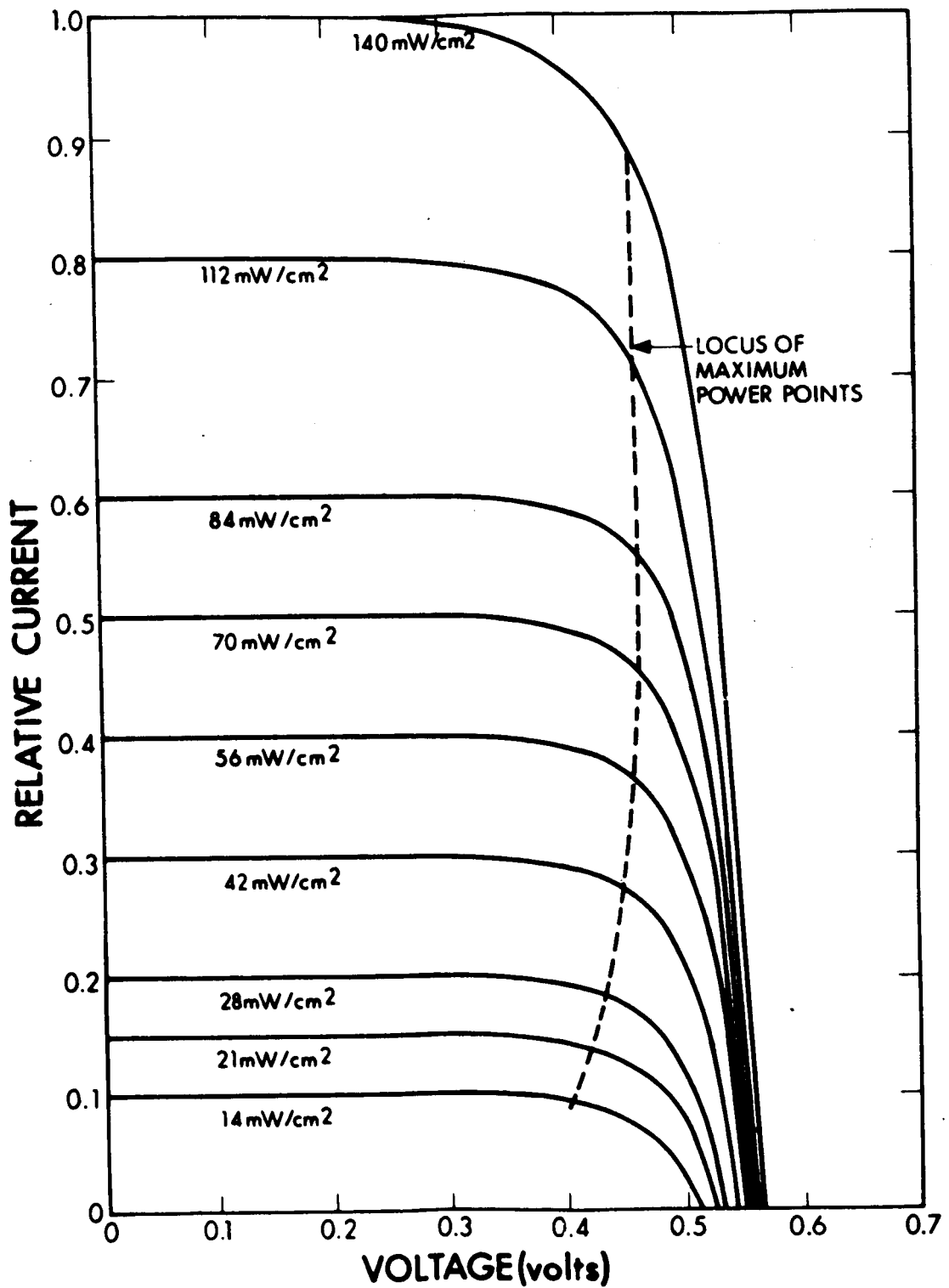


Figure 3-14. Typical I-V Characteristics as a Function of Solar Irradiation at Constant Temperature



The submodule output corrected for the Tedlar film coating and fabrication allowance:

Tedlar film coating	- 1%
Fabrication allowance	- 2%
Total	- 3%

Submodule output:

715.2 (0.97) = 694 mA at 483 mV

Circuit output = 694 mA at 28.0V  
(at 1 AU, 28°C)

The Martian mission has been established as 1 earth year, approximately equivalent to the time period from Martian spring through fall, as defined by the northern hemisphere. Figure 3-15 shows the seasonal position of Mars, and Figs. 3-16 and 3-17 show the inclination of Mars with respect to the Sun.

The attenuation of the Mars atmosphere was assumed to be a logarithmic function of pressure. By analogy with earth conditions, we assigned a transmission factor of 0.7 at a pressure of 1000 mb (earth AMI). The transmission factor at 1 mb was assumed at 1.0. By logarithmic extrapolation, the transmission factor at Mars surface (7 mb) was found to be 0.92. (Reference Fig. 3-18 and the first quarterly report, Subsection 2.1.4.) We believe this transmission factor to be conservative; however, it has been established as a baseline for the program.

The Mars surface solar intensities are:

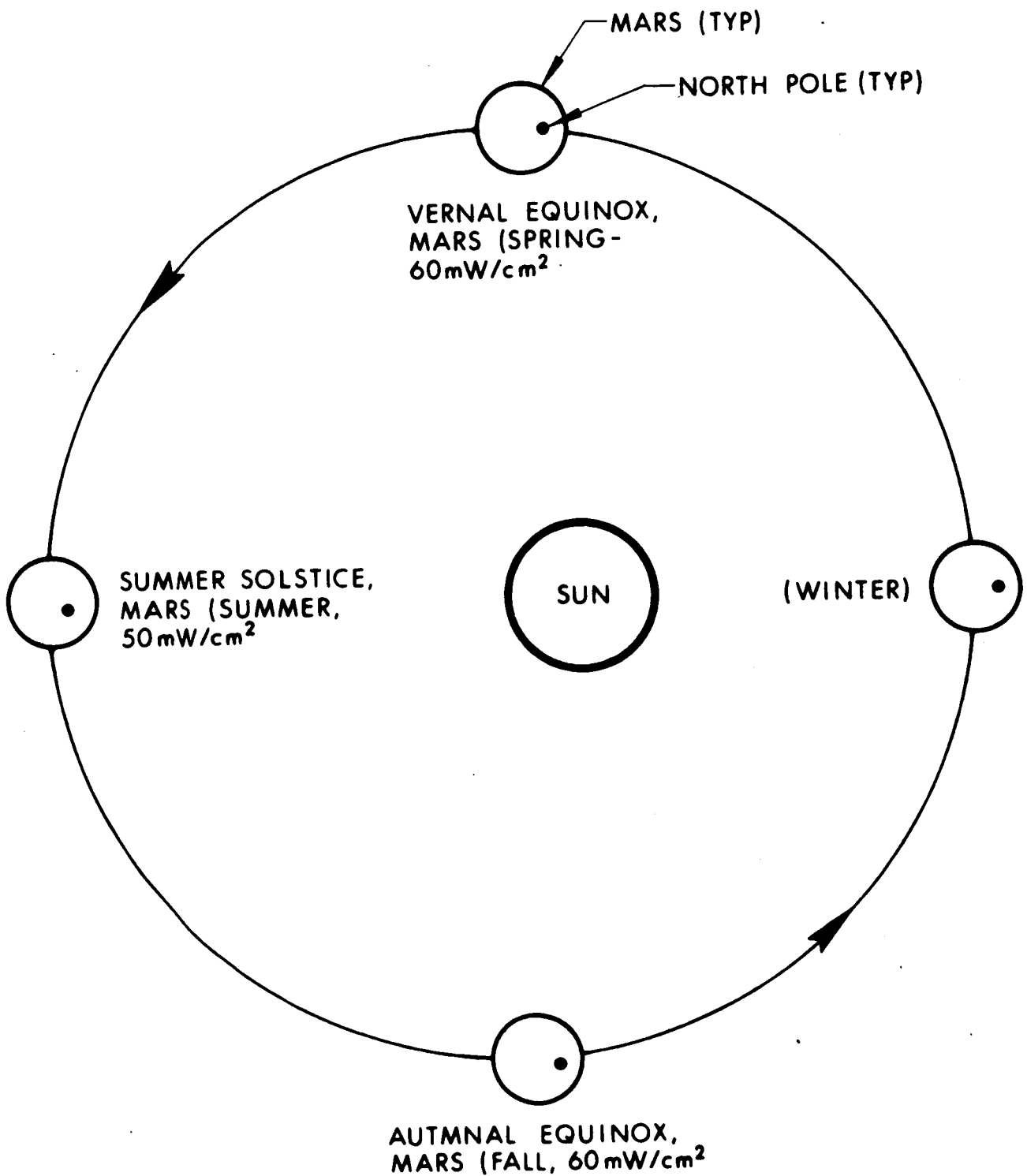
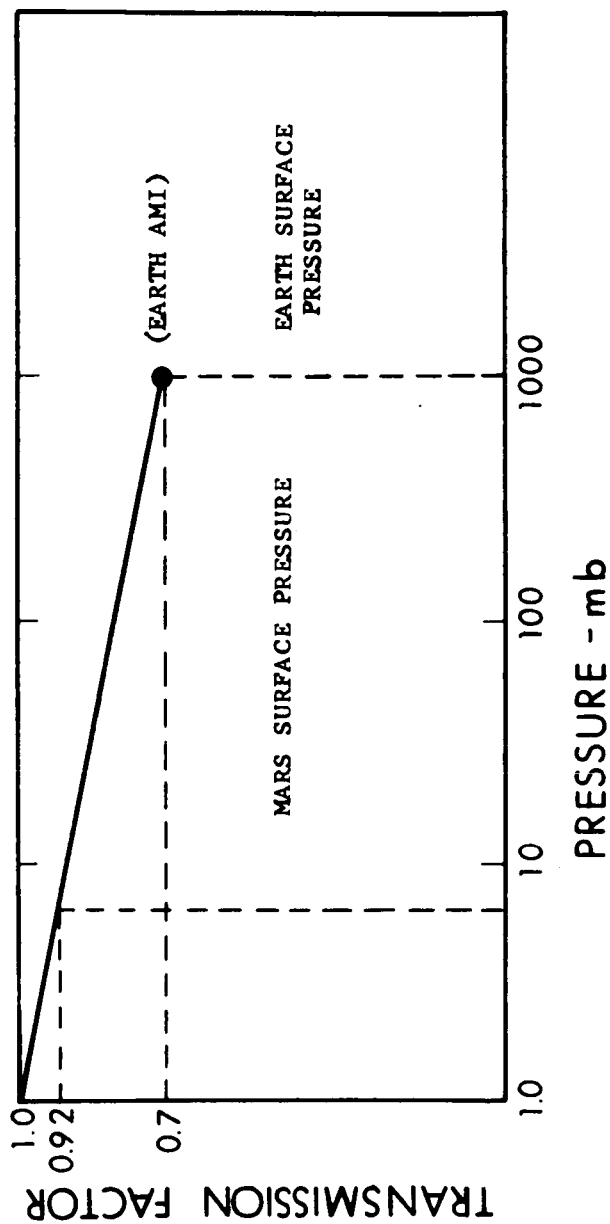


Figure 3-15. Positions of Mars During 1 Earth Year of Planetary Array Operation

- NEAR MARS SPACE: 50 TO 74  $\text{mW}/\text{cm}^2$
- AT MARS SURFACE:  
RECOMMENDED TRANSMISSION FACTOR AT AIR MASS ONE = 0.92
- RATIONALE:



- JUSTIFICATION:
  - a) ONLY GAS MOLECULE SCATTERING CAN BE COMPUTED
  - b) WATER VAPOR SCATTERING - UNKNOWN
  - c) DUST SCATTERING - UNKNOWN
  - d) WATER VAPOR ABSORPTION - UNKNOWN
  - e)  $\text{CO}_2$  ABSORPTION CAN BE CALCULATED, BUT IT MAY BE NEGLECTED AS IT OCCURS AT LONG WAVELENGTHS (  $> 2.5 \mu$  )

Figure 3-18. Mars Solar Intensity

Spring and fall:

$$(60 \text{ mW/cm}^2) (0.92) = 55.2 \text{ mW/cm}^2$$

$$\text{Ratio to AMO} = 55.2/140 = 0.394$$

Summer:

$$(50 \text{ mW/cm}^2) (0.92) = 46.0 \text{ mW/cm}^2$$

$$\text{Ratio to AMO} = 46.0/140 = 0.329$$

Current output per circuit at Mars AMI,  $28^{\circ}\text{C}$  normal to the sun:

Spring and fall:

$$(694 \text{ mA}) (0.394) = 273.4 \text{ mA}$$

Summer:

$$(694 \text{ mA}) (0.329) = 228.3 \text{ mA}$$

Power output:

Spring and fall:

$$273.4 \text{ mA at } 28.0\text{V} = 7.66\text{W}$$

Summer:

$$228.3 \text{ mA at } 28.0\text{V} = 6.39\text{W}$$

The actual power output of the single panel oriented array at noon is a function of a number of variables; these are:

- a. Martian seasonal change in solar intensity, as a function of Mars-Sun distance.
- b. Temperature of the solar array, as a function of season.

It is not the intent of this report to analyze all the possible power output combinations. However, certain limiting conditions will be reviewed in detail, and it will be possible, by extrapolation, to estimate the power for any set of conditions.

The object of the single panel oriented solar array is to provide a three-axis tracking capability, satisfying the packaging restraints imposed by JPL. The deployment of the solar panel and antenna on a vertical boom eliminates the possibility of shadowing from the spacecraft body and antenna. With no shadowing, the array can be made utilizing only 30 circuits to obtain the required output.

The temperature of the array affects the power output, and will vary during the day for any given location and season. A detailed thermal analysis is presented in Section 5; however the following average limiting conditions are cited for reference:

a. Oriented solar panel average temperatures. ( $\pm 20^\circ$  Lat.)

1. First day of spring or fall:

Dawn -  $10.1^\circ\text{C}$   
Noon -  $24.6^\circ\text{C}$   
Sunset -  $20.5^\circ\text{C}$

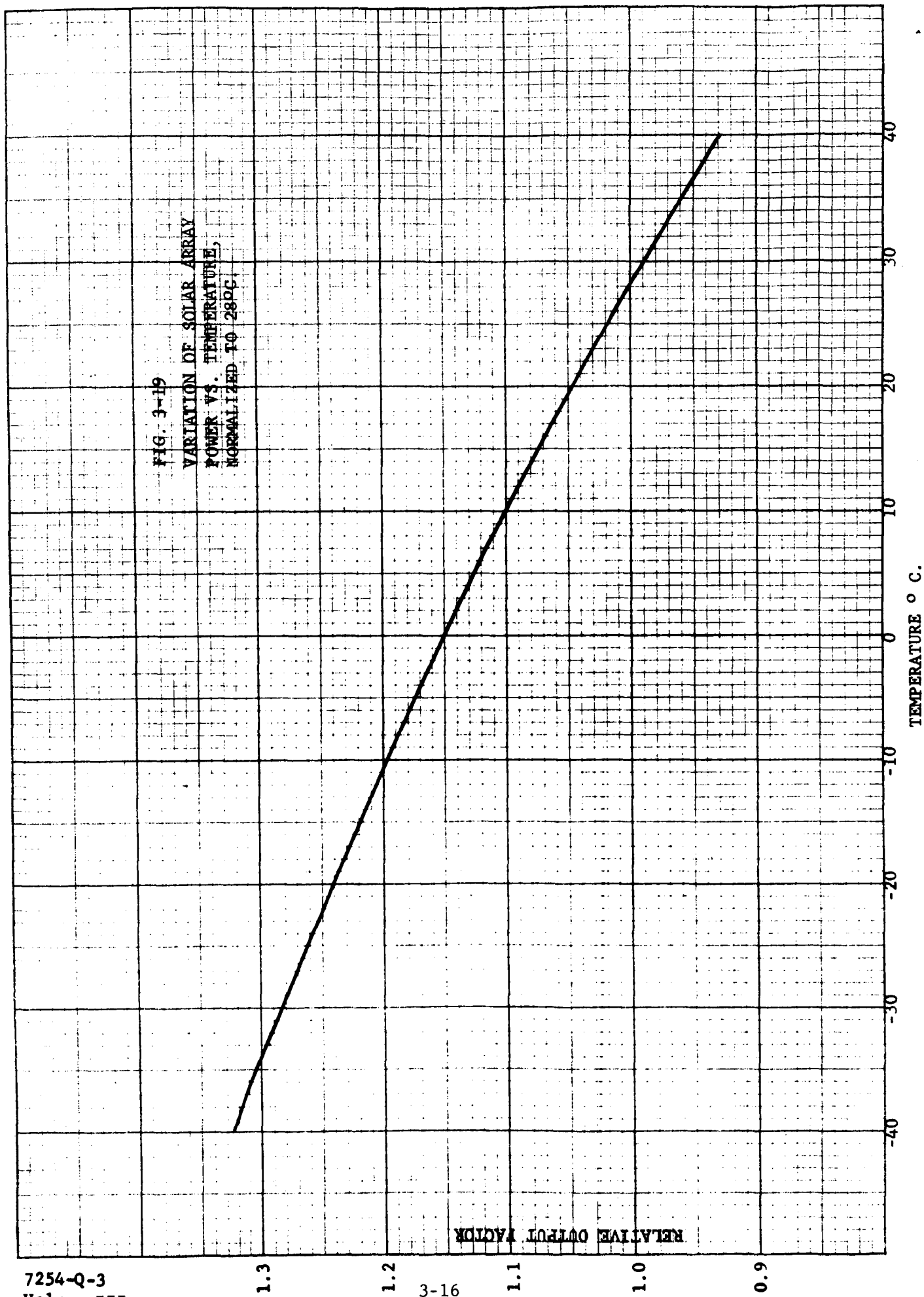
2. First day of summer:

Dawn -  $0.2^\circ\text{C}$   
Noon -  $15.3^\circ\text{C}$   
Sunset -  $11.0^\circ\text{C}$

The power per circuit previously calculated for an estimated temperature at noon of  $28^\circ\text{C}$  can be corrected by the graph, Fig. 3-19. Therefore the power output of a circuit at summer noon, temperature  $15.3^\circ\text{C}$ , is as follows:

$$6.39 (1.073) = 6.856\text{W}$$

FIG. 3-19  
 VARIATION OF SOLAR ARRAY  
 POWER VS. TEMPERATURE,  
 NORMALIZED TO 28°C.



The minimum power output of the array at summer noon, with 30 circuits operating, would be:

$$6.85W (30) = 205.7W$$

The correction for the circuit power at spring or fall noon to a temperature of  $24.6^{\circ}C$  would be:

$$7.66 (1.02) = 7.813W.$$

The power output of the array at noon for the spring or fall seasonal conditions would be:

$$7.813W (30) = 234.4W.$$

The power output at noon for the limiting conditions exceeds the 200W minimum requirement.

The power output of the array fully oriented for a 12-hour daylight period (first day of summer) is affected by two variables. One is the change in temperature from sunrise to sunset; the other is the attenuating effects of the change in air mass for the same time period.

The temperature limits were given previously, and the air mass can be approximated for  $\pm 20^{\circ}$  latitude from the equator by equation:

$$A = [(R + H)^2 - R^2 \sin^2 \theta]^{1/2} - R \cos \theta$$

where

A = air mass as a function of H

R = radius of Mars (miles)

H = atmosphere height of Mars (miles)

$\theta$  = angle of rotation of Mars from solar noon ( $\pm 90^{\circ}$ )

The mean radius of Mars is fairly well established at 2100 miles; however, the atmosphere height of Mars is not known at the present. For the purpose of this report the atmospheric height of zero wind of 90,000 ft, taken from the wind predictions of estimated Voyager data furnished by JPL, will be doubled to give a maximum atmospheric height of 180,000 ft, or approximately 34 miles. Therefore, the ratio of  $R/H = 62$ . By substituting  $R = 62 H$  into the equation for A the following values are obtained:

<u><math>\theta</math> (time)</u>	<u>A</u>
0 (noon)	1.00
15° (1 hr)	1.04
30° (2 hrs)	1.15
45° (3 hrs)	1.42
60° (4 hrs)	1.95
75° (5 hrs)	3.52
90° (6 hrs)	11.20

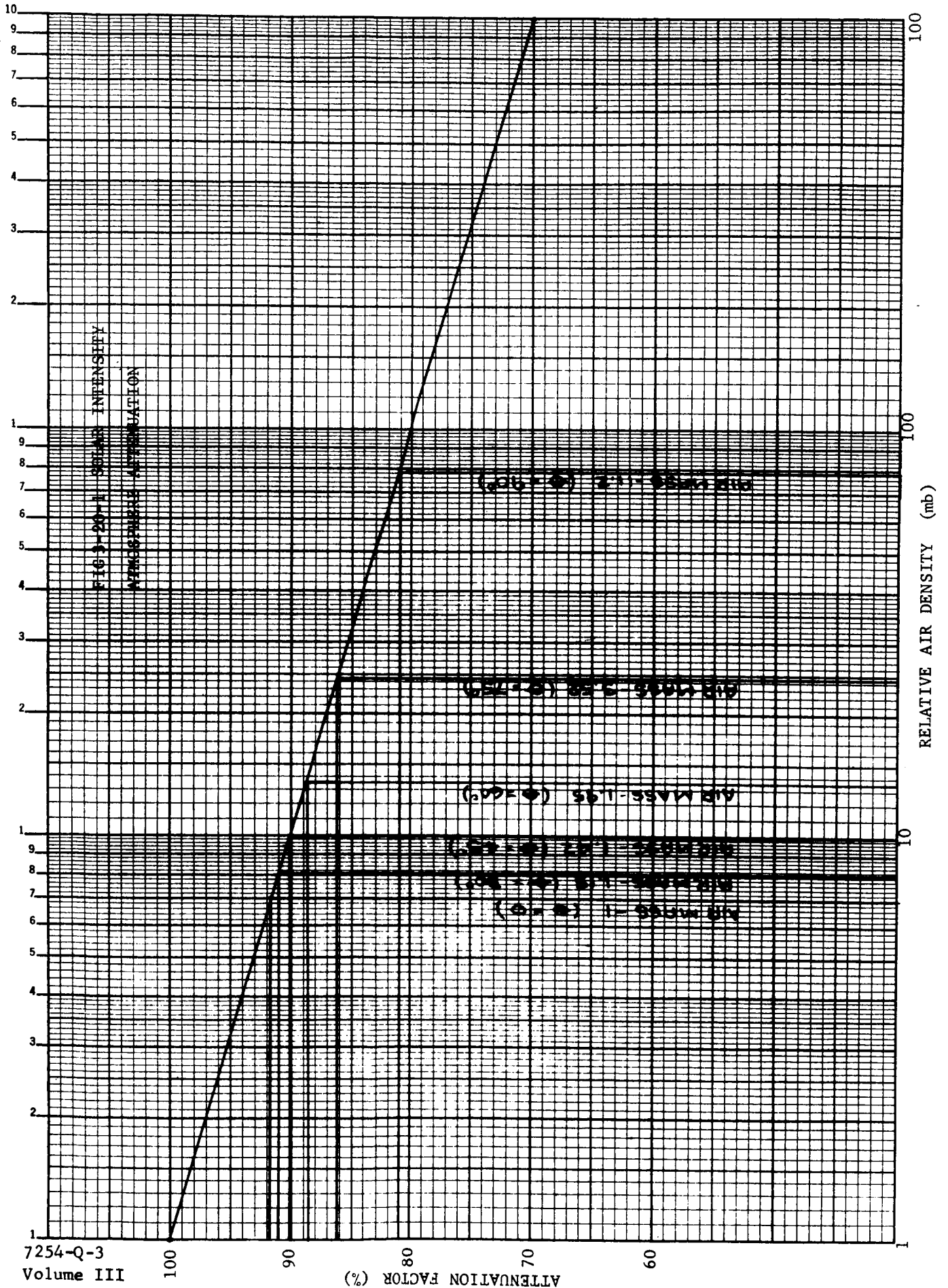
The effect of the air mass attenuation can be seen from the graph (Fig. 3-20-1) which is taken from the analysis presented in Fig. 3-18 of this report.

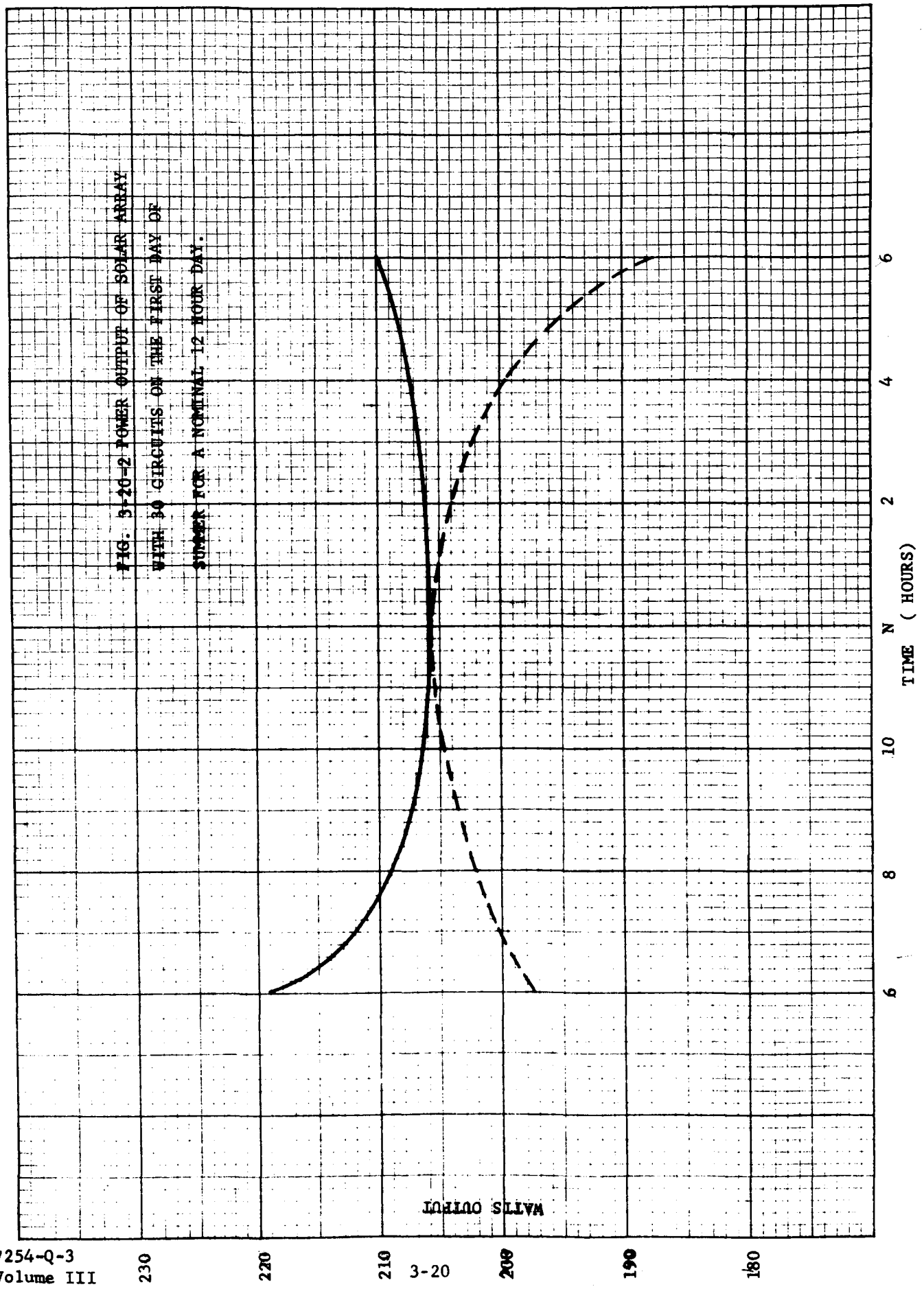
The panel power output for a 12-hour day (first day of summer) at the minimum seasonal solar intensity is plotted in Fig. 3-20-2. The solid line is the panel output corrected for temperature only, and the dashed line is the combined temperature and air mass corrected curve.

### 3.6 MAGNETIC FIELD ANALYSIS

An analysis was made to estimate the magnitude of the magnetic field created by the current carrying circuits of the solar array. The field resulting from the magnetization of materials is absent since all the array materials are nonmagnetic.







The single panel-oriented array has 30 circuits, each circuit consisting of 6 cells in parallel by 60 cells in series. The maximum power per circuit occurs at noon conditions at spring and fall seasons of Mars, and at 28°C it is:

7.66W at 28.0V  
or, 0.274A at 28.0V

Each circuit is reversed in direction on the panel to form a minimum area current loop. The bus wire connections are made with twisted wire pairs to minimize the magnetic field effects. Figure 3-21 shows a typical circuit arrangement.

A calculation of the magnetic field can be effected by considering a pair of adjacent circuits as a current loop whose dipole moment is given by:

$$m = IA \quad (1)$$

where  $m$  is the dipole moment directed from the center of the loop and perpendicular to the plane of the loop;  $I$  is the circulating current; and  $A$  is the area of the loop in square meters. In the rationalized MKS units, the dipole moment is in amp-meter<sup>2</sup>.

The magnetic field due to the dipole at a point  $P$  can be divided into two components. Refer to Fig. 3-22.

$$B_r = \frac{\mu m}{2\pi r^3} (\cos\phi) \quad (2)$$

$$B_\phi = \frac{\mu m}{4\pi r^3} (\sin\phi) \quad (3)$$

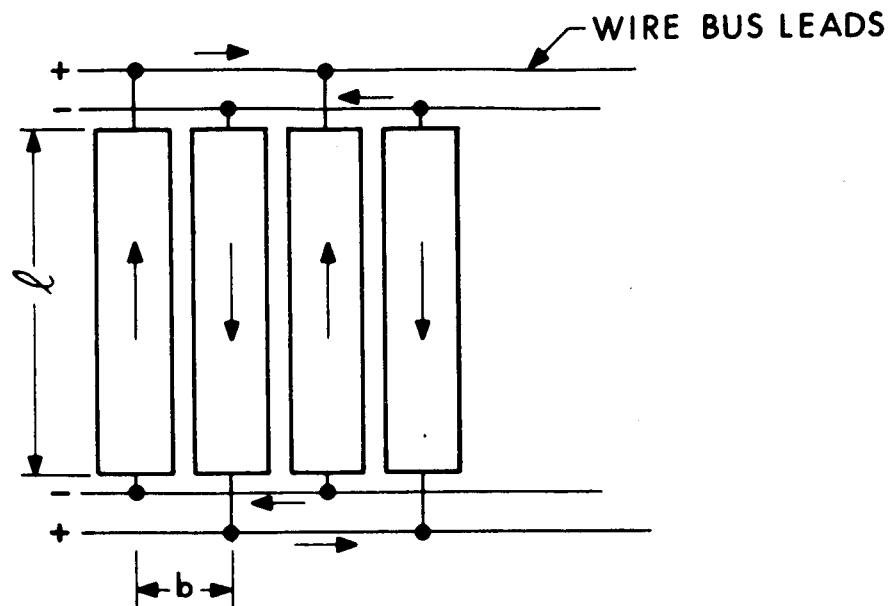


Figure 3-21. Bus and Circuit Arrangement

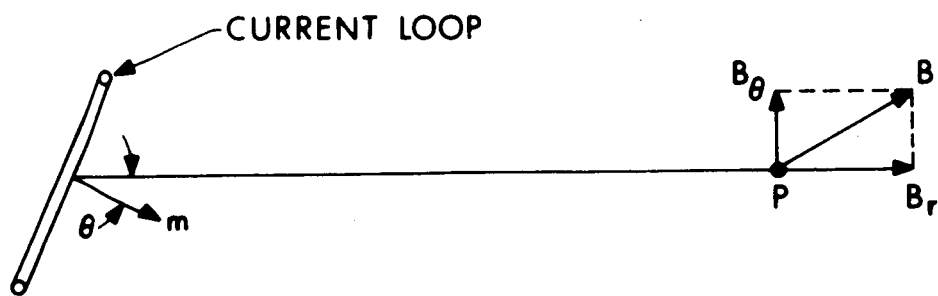


Figure 3-22. Coordinates of Dipole Field

Equations 2 and 3 are valid approximations when the characteristic dimension of the loop is small compared to the distance  $r$ .

The magnetic field at any point can be calculated by applying the three equations to the current loop formed by two adjacent circuits. The resultant field is the vector summation of the contribution of each individual loop. We shall assume that the instruments which are sensitive to the magnetic field are mounted in or near the spacecraft structure. Because the exact location of these instruments have not been specified we shall select a spot in the geometric center of the spacecraft with respect to the solar panels in order to illustrate the order of magnitude of the field. This is the same spot selected in the Type 2 solar panel analysis.

#### 3.6.1 MAGNETIC FLUX CALCULATION

The third array concept differs from the previous two in that there is essentially only one panel. Therefore, the field can never be zero due to symmetry. The worst case condition will be reviewed, i.e., when the panel is closest to the selection spot "P" as shown in Fig. 3-23. For this condition  $B_\theta$  is zero, because  $\theta = 0$  (Ref. Eq. 3), and the total flux is the vector summation of all 15 magnetic loops of the panel, as shown in Fig. 3-24. Only the left half of the panel is shown since the panel has symmetry about its centerline.

The magnetic field in the plane of the panel, as illustrated by Fig. 3-24, will be determined. Fortunately, because of the symmetry, the sine components cancel out so that  $B_\theta = 0$  as previously stated. All the cosine components can be added directly and all are in the direction of  $B_r$ . Referring to Fig. 3-24, the approximate values will be used.

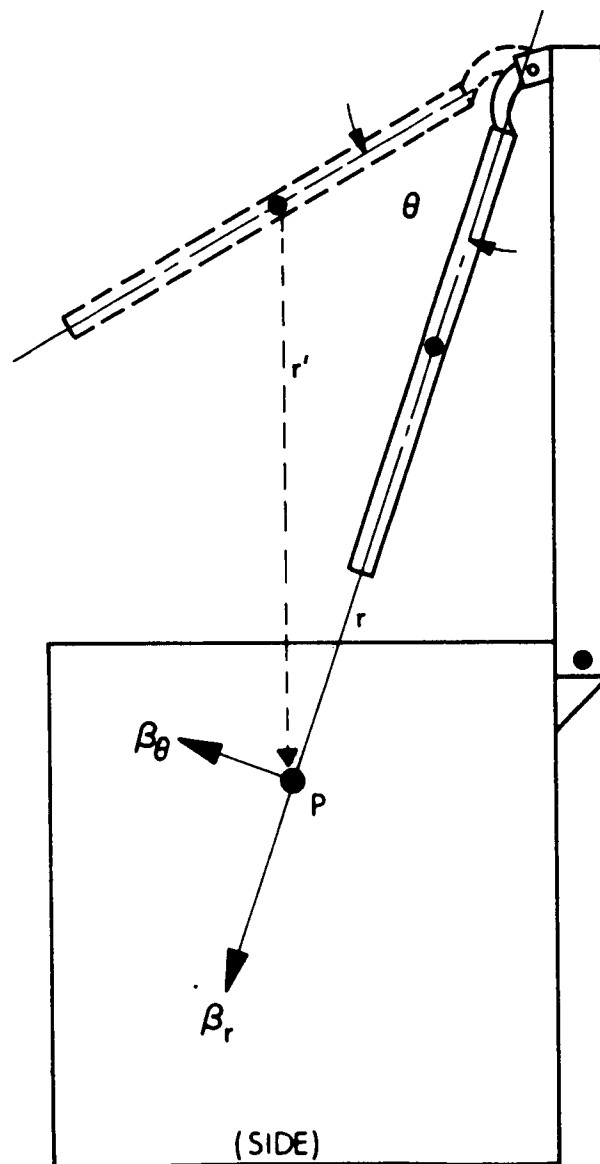


Figure 3-23. Position of Solar Panel with Respect to Magnetic Point P Where Radius  $r$  is a Minimum and  $\theta$  is Zero

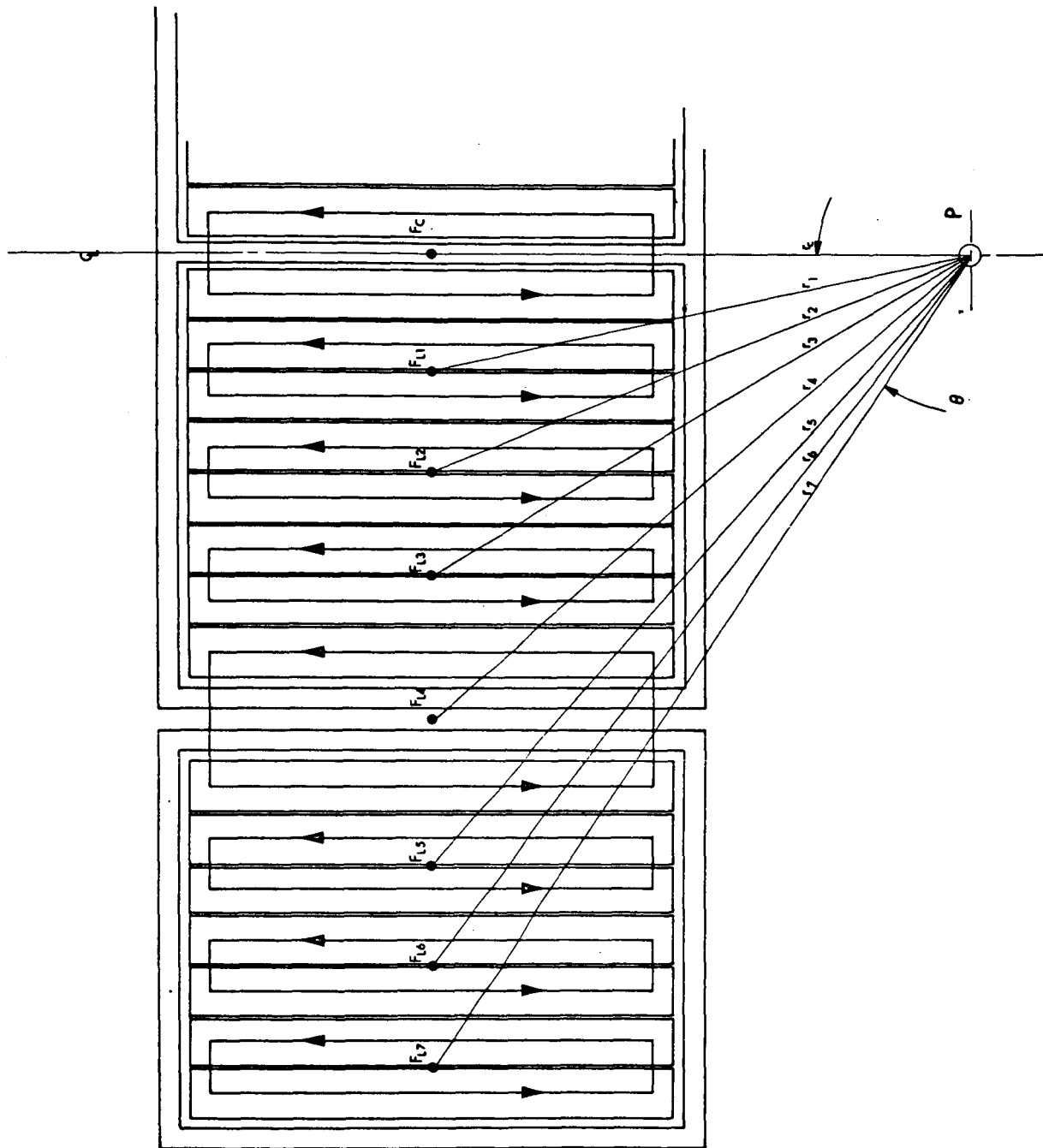


Figure 3-24. Field Vectors Due to Current Loops in Left Half and Center of Panel

$$\begin{aligned}
\mu &= 4\pi \times 10^{-7} \text{ henries/meter} \\
I &= 0.274 \text{ amps} \\
A_c &= 1.22 \times 0.203 = 0.247 \text{ meter}^2 \\
A_{L1-L3} &= 1.22 \times 0.122 = 0.148 \text{ meter}^2 \\
A_{L5-L7} &= 1.22 \times 0.33 = 0.406 \text{ meter}^2 \\
A_{L4} &= 0 \\
\theta_c &= 0 \\
\theta_1 &= 13^\circ \\
\theta_2 &= 23^\circ \\
\theta_3 &= 32^\circ \\
\theta_4 &= 41^\circ \\
\theta_5 &= 49^\circ \\
\theta_6 &= 54^\circ \\
\theta_7 &= 58^\circ \\
r_c &= 53.0 \text{ inches (1.34 meters)} \\
r_1 &= 54.0 \text{ inches (1.37 meters)} \\
r_2 &= 57.0 \text{ inches (1.44 meters)} \\
r_3 &= 61.5 \text{ inches (1.56 meters)} \\
r_4 &= 70.0 \text{ inches (1.78 meters)} \\
r_5 &= 80.0 \text{ inches (2.03 meters)} \\
r_6 &= 87.0 \text{ inches (2.21 meters)} \\
r_7 &= 95.5 \text{ inches (2.42 meters)}
\end{aligned}$$

The total flux at P is equal to:

$$\begin{aligned}
B_{r_T} &= \Sigma \frac{\mu m}{2\pi r_c^3} (\cos\theta_c) + 2 \frac{\mu m}{2\pi r_1^3} (\cos\theta_1) \dots \\
&\quad + \frac{\mu m}{2\pi r_7^3} (\cos\theta_7) \\
&= \frac{4\pi \times 10^{-7} (0.067)}{2\pi (1.34)^3} (1) + \frac{4\pi \times 10^{-7} (0.040)}{\pi (1.37)^3} (0.974)
\end{aligned}$$



$$\begin{aligned}
& + \frac{4\pi \times 10^{-7} (0.040)}{\pi (1.44)^3} (0.920) \\
& + \frac{4\pi \times 10^{-7} (0.040)}{\pi (1.56)^3} (0.848) + \frac{4\pi \times 10^{-7} (0.111)}{\pi (1.78)^3} (0.754) \\
& + \frac{4\pi \times 10^{-7} (0.040)}{\pi (2.03)^3} (0.656) + \frac{4\pi \times 10^{-7} (0.040)}{\pi (2.21)^3} (0.587) \\
& + \frac{4\pi \times 10^{-7} (0.040)}{\pi (2.42)^3} (0.529) \\
& = 5.60 \times 10^{-9} + 6.09 \times 10^{-9} + 4.94 \times 10^{-9} \\
& \quad + 3.58 \times 10^{-9} + 5.88 \times 10^{-9} + 1.25 \times 10^{-9} \\
& \quad + 0.87 \times 10^{-9} + 0.59 \times 10^{-9} \\
& = 28.8 \times 10^{-9} \text{ Weber/meter}^2 \\
& = 28.8 \text{ gamma}
\end{aligned}$$

### 3.6.2 CONCLUSION

The magnetic flux at point P is considerably higher than in the other two arrays analyzed. For comparison, the three values at worst case condition are:

Type I - 8.5 gamma  
 Type II - 3.0 gamma  
 Type III - 28.8 gamma

It should be pointed out that these represent worst case condition for an arbitrarily placed reference point P. Placement of the instrumentation at some other location would alter field intensity, dependent upon location.

## SECTION 4

### STRUCTURAL DESIGN AND ANALYSIS

This section contains the following information:

- a. A functional description of each of the major mechanical components of the vertical boom solar array baseline configuration.
- b. A discussion of the criteria used to select the material for each component.
- c. A description of the mathematical model(s) used to analyze each component.
- d. The loads analysis performed to establish the critical loading condition for each component.
- e. The stress analysis for each component and a summary of the respective margins of safety.
- f. Conclusions and recommendations.

The mechanical components of the array are:

- a. Substrate and framing
- b. Vertical boom
- c. Launch support truss

#### 4.1 SUBSTRATE

##### 4.1.1 DESCRIPTION

There are four substrates required per solar array. However, it is considered essentially as one panel. The center section consists of two spherical, hollowcore substrates, with beryllium edge beams, sharing a common center beam. The center or main substrate is approximately 86.6 x 54.0 inches with a plan area of 32.5 ft<sup>2</sup>. The folding side panels

are of identical construction, and are mounted by hinges to the ends of the center substrate. Each side substrate is approximately 39.2 x 54 inches, with a plan area of 14.7 ft<sup>2</sup>, making a total panel area of 61.9 ft<sup>2</sup>. All substrates are aluminum and spherical, and have hollow-cores. "H" film dielectric is bonded to the cell side, and they all have a common spherical radius of 155.5 inches. All substrates are contained by beryllium tube frames which retain the boundary of the spherical hollowcore to establish shell stability. The center panel has the solar cells mounted on the convex side of the hollowcore. The side panels have the solar cells mounted on the concave side.

#### 4.1.2 MATERIAL SELECTION

The substrate material chosen for this configuration is electroformed aluminum hollow core. This material was chosen for this application based on the following considerations:

- a. Fabrication: The electroforming fabrication technique eliminates in-process handling of foil gage materials and difficult bonding operations required to produce comparable types of sandwich shell structures.
- b. Weight: The one-piece structure which results from the electroforming process is lighter than laid-up sandwich structures of equivalent stiffness.

#### 4.1.3 MATHEMATICAL MODELS

- a. Dynamic launch load: The model used to calculate the dynamic internal loads during launch assumes a substrate panel which is simply supported along its periphery. The external loads were assumed to act normal to the plane which is tangent to the substrate at its center.
- b. Wind loading: The substrate panels were assumed to be flat plates placed normal to the direction of the wind for worst case loading.

#### 4.1.4 CRITICAL LOAD ANALYSIS

- a. Launch load: The first fundamental resonant frequency of the substrate was determined by using the following equation:

$$f_n = \frac{1}{2\pi} \left[ \frac{g}{\rho h} \left( D \{ \lambda_1^2 + \mu_1^2 \}^2 + \frac{Eh}{R} \right) \right]^{1/2}$$

where:

$$g = 386 \text{ IPS}^2$$

$$\rho h = (\text{hollowcore and dead load wt/area}) = 1.31 \times 10^{-3} \text{ psi}$$

$$E = 7.8 \times 10^6 \text{ psi}$$

$$I = 1.58 \times 10^{-6} \text{ in}^4/\text{in}$$

$$D = EI = 12.32 \text{ lb-in}^2/\text{in}$$

$$\lambda_1 = \pi/\alpha = 5.817 \times 10^{-2}/\text{in} \quad \alpha = 54$$

$$\mu_1 = \pi/\beta = 7.25 \times 10^{-2}/\text{in} \quad \beta = 43.3$$

$$R = (\text{radius of curvature}) = 155.5 \text{ in}$$

$$h' = (\text{effective height based on area})$$

$$= \left[ 2 + \left( \frac{h}{a} \right) - \sqrt{\frac{3}{2}} \left( \frac{d}{a} \right) \right] t$$

where

$$h = 0.10 \text{ in}$$

$$a = 0.525 \text{ in}$$

$$d = 1.00 \text{ in}$$

$$t = 0.004 \text{ in}$$

$$\therefore h' = 2.165 \times 10^{-3} \text{ in}$$

and

$$f_n = \frac{1}{2\pi} \left[ \frac{386}{1.31 \times 10^{-3}} \left( 12.32 \{ 5.817^2 + 7.25^2 \} 10^{-8} + \frac{(7.8 \times 10^6)(2.165 \times 10^{-3})}{1.555^2 \times 10^4} \right) \right]^{1/2}$$

$$f_n = 72.21$$

For an input load of 1.5 g at 72.2 Hz (see 7254-Q-1) the maximum deflection of the substrate occurs at its center and has a magnitude of 0.228 inch which was determined by the following equation:

(See 7027-1DR, 18 May 1966, Appendix E)

$$W = \frac{16}{\pi^2} \frac{Q}{(2\pi fn)^2} \bar{W}(\alpha, \beta) \ddot{W}_s$$

where  $Q$  = dynamic magnification = 50

$\bar{W}$  = 1 (at center of panel)

$W_s$  = sinusoidal input at 72 Hz = 1.5g

$\omega_{11} = 2\pi fn = 453.479$

$$\therefore W = \frac{16(50)(1)(1.5)(386)}{\pi^2 (453.479)^2}$$

$\ddot{W} = 0.224$  inch

The maximum acceleration response at the center of the substrate to an input load of 1.5g is:

$$\ddot{W} = \frac{16}{\pi^2} Q \ddot{W}_s$$

$$\ddot{W} = \frac{16}{\pi^2} (50)(1.5)$$

$$\ddot{W} = 121.6g \text{ (0-peak)}$$

b. Wind Load: The total wind load on a flat plate is given by the relation:

$$F = 1/2 C_D \rho A V^2$$

where      $F$  = total force in lb

$C_D$  = a coefficient depending on aspect ration,  $a/b$ , and the angle between the plate and the wind flow,  $\alpha$

$A$  = total area of plate in  $\text{ft}^2$

$\rho$  = the mass density of the atmosphere (Mars)  $\frac{\text{lb-sec}^2}{\text{ft}^4}$

$V$  = wind velocity in  $\text{ft/sec}$

The specific parameters for the concept being analyzed are:

$a/b$  = 2

$\alpha$  =  $90^\circ$  worst case

$C_D$  = 1.162

$A$  =  $61.9 \text{ ft}^2$

$\rho$  =  $3.59 \times 10^{-5} \text{ lb-sec}^2/\text{ft}^4$

$V$  =  $325 \text{ ft/sec}$  (free stream velocity  $\times 0.67$  + gusts) i.e.,  
 $V = (186 \times 0.67 + 200)$

$F = 1/2 (1.16)(3.59 \times 10^{-5})(61.9)(325)^2$   
 $F = 136.0$

The average pressure on the panel due to the wind loading is  $2.19 \text{ lb/ft}^2$  or  $0.0152 \text{ psi}$ . This average applied pressure is small compared to the equivalent average applied pressure of  $0.159 \text{ psi}$  which results from the random vibration loading. The design load for the panel will be a pressure of  $0.159 \text{ psi}$ .

#### 4.1.5 STRESS ANALYSIS

The membrane force per unit length is determined by

$$\frac{P}{l} = \frac{PR}{2}$$

where  $\frac{P}{\ell}$  = membrane force per unit length - lb/in  
 $R$  = radius of curvature = 155.5 in  
 $\rho$  = (applied pressure) =  $(SpWt)_p \times g$

where  $SpWt$  = (specific weight) =  $1.31 \times 10^{-3}$  psi  
 $g = \ddot{W} = 121.6$  (0-peak) g  
 $\rho = 0.159$  psi  
 $\therefore \frac{P}{\ell} = \frac{(1.159 \text{ psi})(155.5) \text{ in}}{2}$   
 $\frac{P}{\ell} = 12.38$  lb/in.

The average stress (design limit stress) is obtained by the following equation:

$$\sigma = \frac{P}{\ell h}$$

where:  $\sigma$  = average working stress - psi  
 $P/\ell$  = (membrane load per unit length) = 12.38 lb/in  
 $h' =$  (effective height of hollowcore) =  $2.165 \times 10^{-3}$  in  
 $\therefore \sigma = 5731$  psi

The allowable stress for the hollowcore, based on local crippling of the skin, is calculated from the following relation:

$$\sigma = \frac{K \pi^2 E}{12(1 - \nu^2)} \left( \frac{t}{4a - \sqrt{3d}} \right)^2$$

where  $K$  = crippling coefficient = 12 (experimentally determined)  
 $E = 7.8 \times 10^6$  psi  
 $\nu = 0.33$   
 $t = 0.004$  in  
 $a = 0.525$   
 $d = 1.00$   
 $\sigma_{\text{allowable}} = 10,219$  psi

Margin of Safety:

$$M.S. = \frac{\text{allowable stress}}{\text{actual stress} \times F.S.} - 1$$

$$M.S. = \frac{10,219}{5,731 \times 1.25} - 1 = 0.426$$

The critical pressure for overall buckling of the panel is given by

$$P_{cr} = \frac{D(f_n^2 + \mu_m^2)^2 + \frac{Eh}{R^2}}{\frac{R}{2}(f_n^2 + \mu_m^2)}$$

(See 7027-1DR, 18 May 1966, Appendix D, page 9.)

$$P_{cr} = \frac{2(0.7)}{155.5 (70.3311) \times 10^{-4}}$$

$$P_{cr} = 1.28 \text{ psi}$$

The margin of safety of overall buckling of the panel is:

$$M.S. = \frac{\text{critical pressure}}{\text{actual pressure} \times F.S.} - 1$$

$$M.S. = \frac{1.28}{0.159 \times 1.25} - 1$$

$$M.S. = 5.44$$



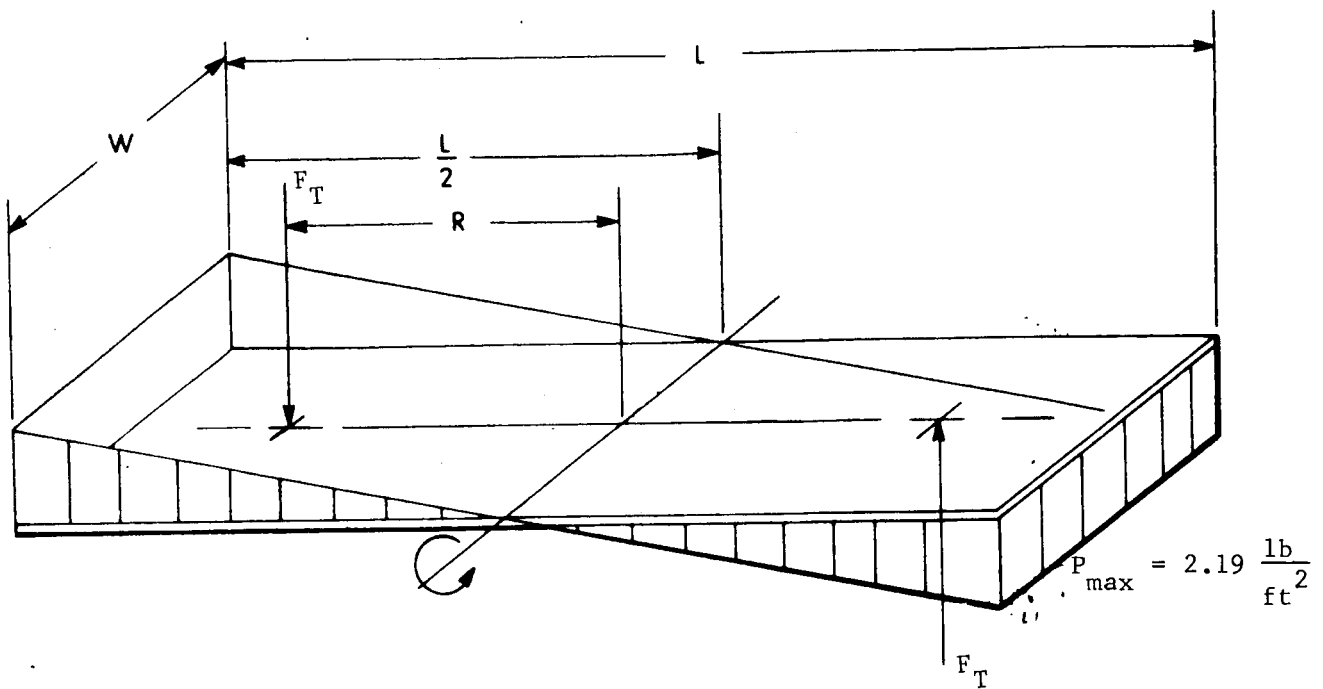


Figure 4-1. Torsional Wind Loading Condition on the Solar Panel

where:

$$L = 170 \text{ inches (14.16 ft)}$$

$$\frac{L}{2} = 85 \text{ inches (7.08 ft)}$$

$$W = 54 \text{ inches (4.5 ft)}$$

$$R = \frac{2}{3} \left( \frac{L}{2} \right) = 36 \text{ inches (3.0 ft)}$$

The maximum bending stress in the boom due to the wind loading is:

$$S = \frac{Mc}{I}$$

where  $M = F(\ell) + M_0$

$$F = 135.5 \text{ lb}$$

$$\ell = 60 \text{ inches}$$

$$M_0 = 333.3 \text{ ft lb (4000 in. lb)}$$

$$C = 2.5 \text{ inches}$$

$$I = \pi R^3 (t)$$

$$R^3 = 15.625$$

$$t = 0.025 \text{ inches}$$

$$S = \frac{[135.5(60) + 4000](2.5)}{\pi (15.625)(0.025)}$$

$$= 24,700 \text{ psi}$$

The critical bending moment based on elastic buckling is:

$$M_{cr} = K \frac{E}{1 - \nu^2} r t^2 \quad (\text{Roark})$$

where  $K = 0.72$  (minimum experimentally determined value)

$$E = 42 \times 10^6$$

$$\nu = 0.1$$

$$r = 2.5$$

$$t = 0.025$$

$$M_{cr} = \frac{(0.72)(42 \times 10^6)(2.5)(0.025)^2}{1 - (0.1)^2}$$

$$M_{cr} = \frac{0.72(42 \times 10^6)(2.5)(0.625 \times 10^{-3})}{0.99}$$

$$= 47,250 \text{ in./lb}$$

The yield strength of the beryllium is lower than the stress produced by the critical bending moment for elastic buckling. Therefore, the allowable stress for the wind loading condition which produces bending in the boom is the yield stress.

The margin of safety for the bending load is

$$M.S. = \frac{\text{yield strength}}{\text{maximum bending stress} \times 1.25} - 1$$

$$M.S. = \frac{58,000}{24,700 \times 1.25} - 1 = 0.878$$

The stress in the boom due to the torsional loading, Ref. Fig. 4-1, is as follows:

$$S_s = \frac{M_o (16)}{\pi d^3 \left(1 - \frac{d_1^4}{d^4}\right)}$$

where:  $M_o = 406.5 \text{ ft lb (4878 in. lb)}$

$d = 5.000 \text{ inches}$

$d_1 = 4.950 \text{ inches}$

$$S_s = \frac{4878 (16)}{\pi (125) \left(1 - \frac{121.289}{125.000}\right)}$$

$$= 6,860 \text{ psi}$$

The critical stress based on elastic buckling due to the torsional load is

$$S_{cr} = 0.272 \frac{E}{(1 - \nu^2)^{3/4}} \left(\frac{2t}{d}\right)^{3/2} \quad (\text{Roark})$$

where

$$\begin{aligned} E &= 42 \times 10^6 \\ U &= 0.1 \\ t &= 0.025 \\ d &= 5.000 \end{aligned}$$

$$\begin{aligned} S_{cr} &= \frac{0.272(42 \times 10^6)(0.00316)}{0.992} \\ &= 36,400 \text{ psi} \end{aligned}$$

The allowable buckling stress is lower than the shear stress of the material(55,000 psi), and therefore determines the margin of safety of the boom.

The margins of safety of the vertical boom for the torsional wind loading condition is

$$\begin{aligned} \text{M.S.} &= \frac{S_{cr}}{S_s (\text{FS})} \\ &= \frac{36,400}{6,860 (1.25)} \\ &= 4.25 -1 \end{aligned}$$

$$\text{M.S.} = 3.25$$

The rotational deflection of the boom due to torsional wind loading is given by

$$\theta = \frac{M_o L}{KG}$$

where  $M_0 = 406.5 \text{ ft lb (4878 in. lb)}$   
 $L = 60 \text{ inches}$   
 $K = 1/2 \pi r^3 t$   
 $r = 2.5 \text{ inches}$   
 $t = 0.025 \text{ inches}$   
 $G = \text{shear modulus} = 20 \times 10^6 \text{ psi}$

$$\begin{aligned}\theta &= \frac{4878 (60)(2)}{(20 \times 10^6)(\pi)(15.625)(0.025)} \\ &= \frac{292,680}{(20 \times 10^6)(1.226)} \\ &= 0.0119 \text{ rad}\end{aligned}$$

$$\theta = 0.681 \text{ degrees}$$

#### CONCLUSION

The boom is sized by the rotational stiffness criteria to limit the rotation deflection under the torsional wind loading conditions. This is necessary to provide a stable mounting for the communication antenna, which is combined with the solar array mounting in this design. This analysis assumes that the boom is cantilevered from a rigid base. Further analysis of the boom deflection and dynamic response should include the effects of the elasticity and tolerances in the boom latch mechanism, and the elasticity of the spacecraft body.

#### 4.2.2 LAUNCH SUPPORT TRUSS

The truss which supports the rotating boom is shown schematically in Figure 4-2. The truss is designed to use beryllium tubes fabricated from cross-rolled sheet.

Each solar panel section is latched to the spacecraft body during launch so that the effective dead load on the support truss in the Z direction is as summarized below.

Panel - 15.698 (0.5)	=	7.849
Vertical Boom - 1.530 (0.5)	=	0.765
Motors (0.500) (2)	=	1.000
Motor Drives (1.000) (2)(0.5)	=	1.000
Sun Sensor	=	0.100
Antenna Assembly	=	<u>3.500</u>
	F	= 14.214

The fundamental resonant frequency of the support truss can be estimated from the following relation

$$f_n = \frac{1}{2\pi} \sqrt{\frac{g}{D_z}}$$

where  $D_z$  is the vertical static displacement produced by the effective dead load.  $D_z$  is determined as shown below.

$$\begin{aligned}\vec{F}_{AB} + \vec{F}_{CB} + \vec{F}_{DB} + \vec{F} &= 0 \\ \vec{F}_{AB} &= \frac{F_{AB}}{71.00} (58 \hat{i} + 32 \hat{j} + 25 \hat{k}) \\ \vec{F}_{CB} &= \frac{F_{CB}}{71.00} (58 \hat{i} - 32 \hat{j} + 25 \hat{k}) \\ F_{CB} &= \frac{F_{CB}}{61.6} (60 \hat{i} - 14 \hat{k}) \\ F &= -14.214 (\hat{k})\end{aligned}$$

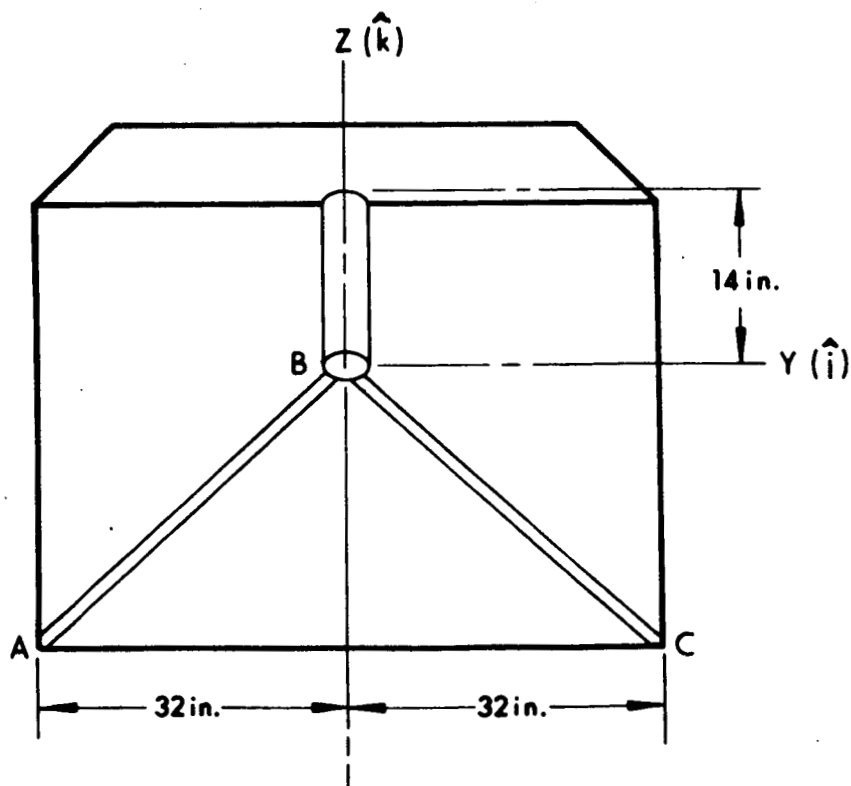
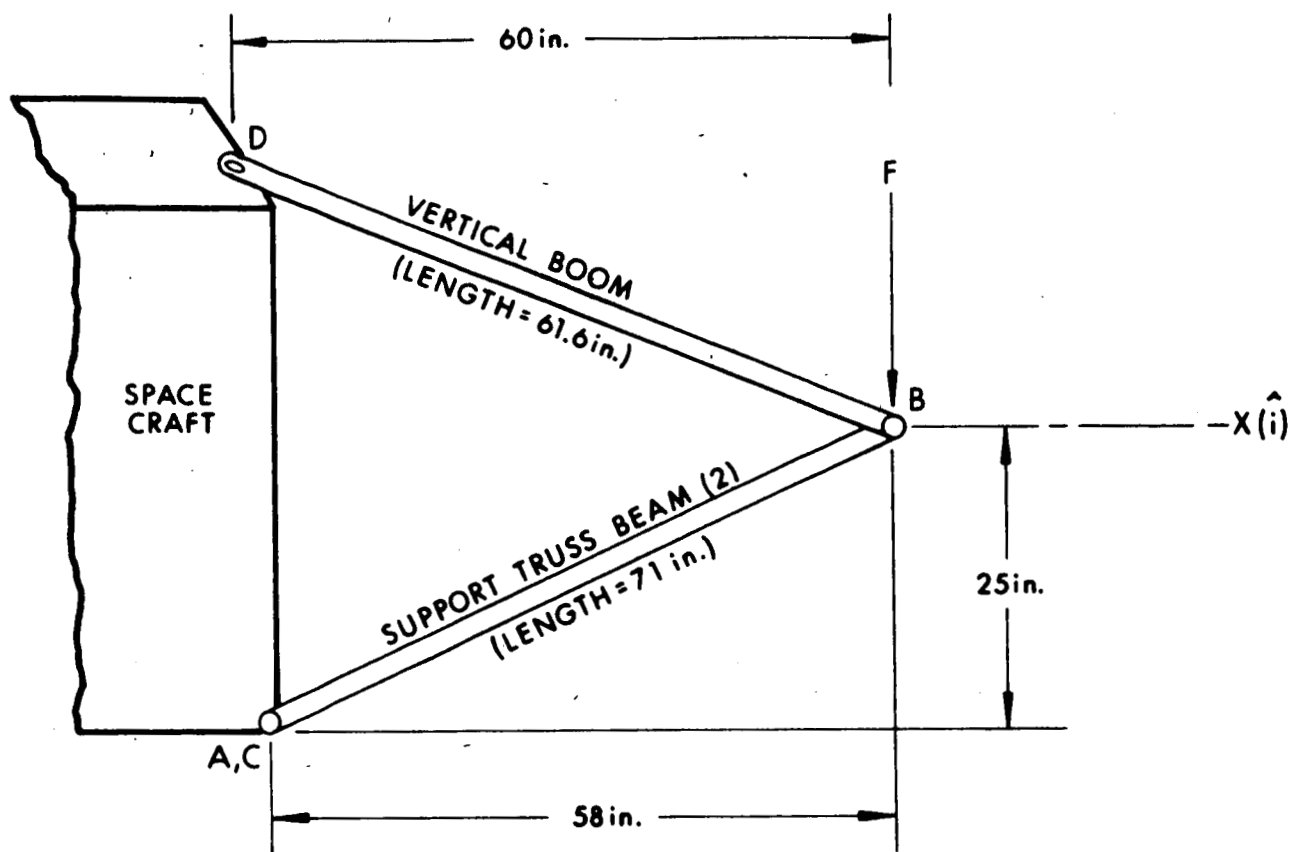


Figure 4-2. Launch Loading Conditions

$$\begin{bmatrix} 58 & 58 & \frac{(71)(60)}{61.6} \\ 32 & -32 & 0 \\ 25 & 25 & -\frac{14(71)}{61.6} \end{bmatrix} \begin{bmatrix} F_{AB} \\ F_{CB} \\ F_{DB} \end{bmatrix} = \begin{bmatrix} 0 \\ 0 \\ 14.214 (71.00) \end{bmatrix}$$

$$F_{AB} = \frac{\begin{bmatrix} 0 & 58 & \frac{71(60)}{61.6} \\ 0 & -32 & 0 \\ \frac{14.214(71)}{1.705 \times 10^5} & 32 & \frac{14(71)}{61.6} \end{bmatrix}}{1.705 \times 10^5} = \frac{(14.214)(71)(32)(71)(60)}{1.705 \times 10^5 (61.6)}$$

$$F_{AB} = (0.92138)(F) = 13.09 \text{ lb}$$

$$F_{CB} = F_{AB} = 13.09 \text{ lb}$$

$$F_{DB} = \frac{-2(58)(32)(71)(14.214)}{1.705 \times 10^5} = -1.5458(14.214)$$

$$F_{DB} = -1.5458(F) = 21.97 \text{ lb}$$

#### TABULATION OF CALCULATION OF VERTICAL DEFLECTION, $D_Z$

Member	Area, A (in <sup>2</sup> )	Length, L (in)	F (lb)	$e = \frac{FL}{AE}$	Unit Load, $P_Z$ (lb/lb)	$P_Z(e)$ (in.)
AB	0.100	71.0	-13.09	-0.000221	-0.92138	0.000203
BC	0.100	71.0	-13.09	-0.000221	-0.92138	0.000203
BD	0.393	61.6	21.97	-0.000082	1.5458	0.000126

$$D_Z = \Sigma P_Z(e) = 0.000532$$



The natural frequency is:

$$f_n = \frac{1}{2\pi} \sqrt{\frac{386}{0.000532}} = \frac{10^3}{2\pi} \sqrt{0.72556}$$

$$= 135.6 \text{ cps}$$

From Fig. 4-3, the input acceleration for the main structure at 135.6 cps is 4.6 g (0-peak).

Applying a 4.6 g input with a Q of 20 gives the following dynamic loads in the main truss members,

$$F_{AB} = F_{CB} = 1204.3 \text{ lb}$$

$$F_{BD} = 2021 \text{ lb}$$

These loads are alternate tension-compression loads.

The critical loads for Euler buckling are given by:

$$F_{cr} = \frac{\pi^2 E I}{L^2}$$

$$F_{cr(AB)} = \frac{\pi^2 (42 \times 10^6) (\pi) (1)^3 (0.016)}{(71.0)^2}$$

$$F_{cr(AB)} = 4132 \text{ lb}$$

$$F_{cr(BD)} = \frac{\pi^2 (42 \times 10^6) (\pi) (2.5)^3 (0.025)}{(61.61)^2} = 134,000 \text{ lb}$$

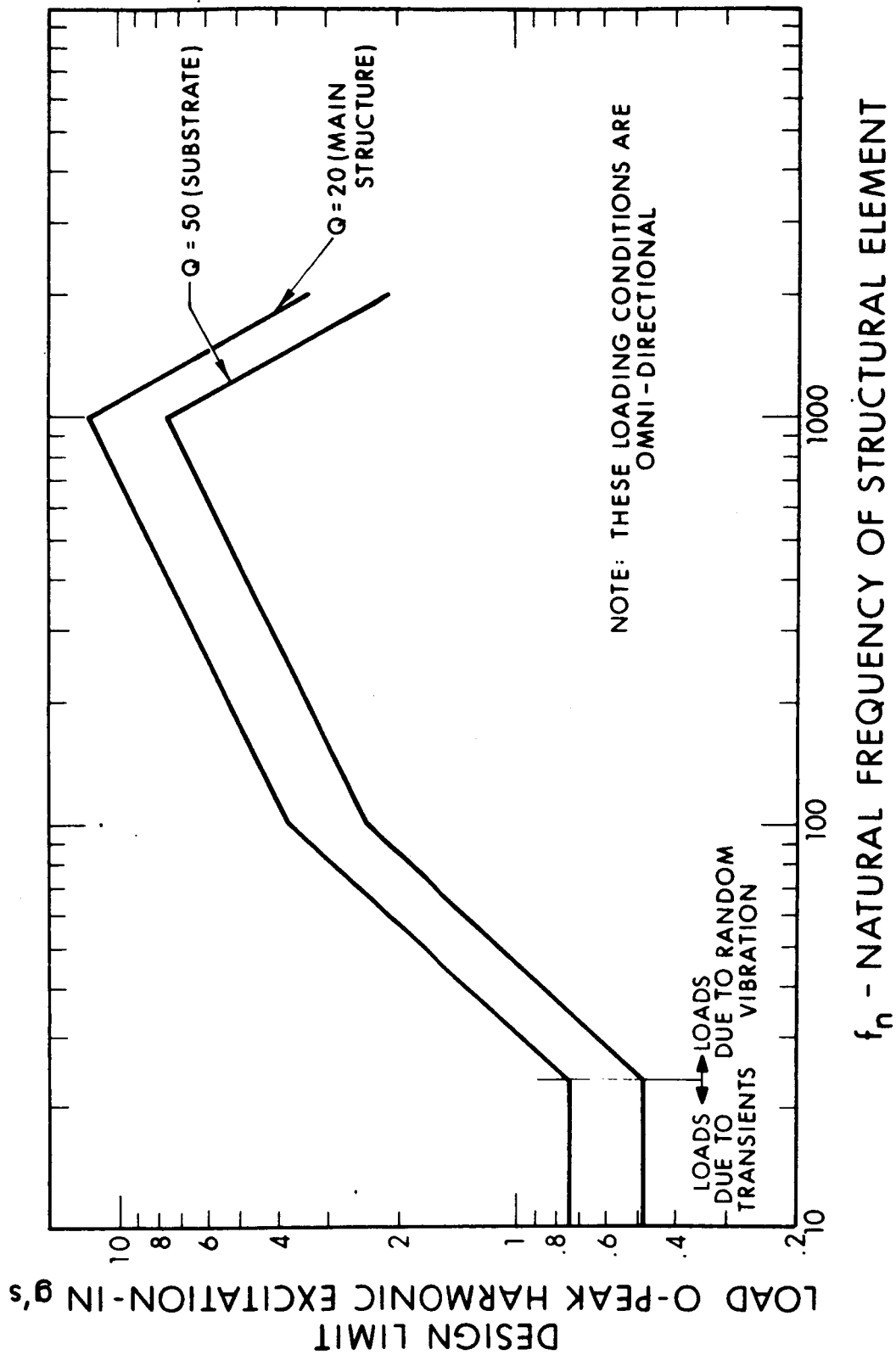


Figure 4-3. Design Loads for Launch Configuration

The margins of safety are:

$$M.S. = \frac{S_{cr}}{S(FS)} - 1$$

$$\begin{aligned} M.S. \begin{matrix} (AB) \\ (BC) \end{matrix} &= \frac{4132}{(1204.3)(1.25)} - 1 \\ &= 1.74 \end{aligned}$$

Member BD is not critical in Euler buckling.

The margins of safety are sufficient for the members, for the buckling loads imposed.

The local resonant frequency of the diagonal member of the support is

$$f_n = 1.57 \sqrt{\frac{EI}{\rho L^4}}$$

where:  $E = 42 \times 10^6$  psi

$I = \pi R^3(t) = 0.0503$

$\rho = \frac{0.079}{g} = 1.7055 \times 10^{-5} \frac{\text{lb sec}^2}{\text{in.}^2}$

$L = 71.0$  in.

$$f_n = \frac{1.57 \times 10^3}{5041} \sqrt{\frac{42(0.0503)}{1.7055 \times 10^{-5}}}$$

$$f_n = 109.6 \text{ cps}$$

From Fig. 4-3, the input acceleration for the structure at 109.6 cps is 4.0 g.

The maximum bending moment in the beam due to local resonance is

$$M = \frac{4}{\pi^3} \ddot{\delta} \rho Q L^2$$

where  $\ddot{\delta} = (4.0)(386)$

$$Q = 20$$

$$M = \frac{4}{\pi^3} (4.0)(386)(1.7055 \times 10^{-5})(20)(5041)$$

$$= 342.4 \text{ in.-lb}$$

The bending stress is

$$S_B = \frac{Mc}{I} = \frac{342.4(1)}{0.0503} = 6,807 \text{ psi}$$

The margins of safety on yield and buckling for this loading condition are high.

#### CONCLUSION

The support truss is sized to support the boom and array assembly during launch conditions. The landing shock is small compared to the launch conditions. After deployment of the array, the support truss is released and falls away, pivoting on its mounting to the spacecraft. It is not a part of the operational structure.

SECTION 5  
SYSTEM ANALYSIS

5.1 ENVIRONMENTAL INTERACTIONS

5.2 MATERIAL EVALUATION

} Refer to Volume I

5.3 THERMAL ANALYSIS

Refer to Volume II

5.4 WEIGHT ANALYSIS, SINGLE-PANEL-ORIENTED ARRAY

The weight breakdown for the single-panel-oriented array is given in Table 5-VI.

5.5 RELIABILITY CONSIDERATIONS FOR THE TWO-AXIS VERTICALLY-MOUNTED ARRAY

5.5.1 PHYSICAL DESCRIPTION

The array consists of four individual solar panels deployed as shown in drawing 7254-119.\* Each of the panels consists (electrically) of submodules having six parallel cells each. A total of 60 submodules are series-connected to form one circuit. Thirty circuits are parallel-connected to provide the required power output for the array. To provide electrical isolation between panel and output load, a pair of redundant diodes is connected to the output of each circuit. The purpose is to provide protection to the satellite power system in event of a short to the substrate of any section. The probability of a failure mode of this type occurring is minimal.

---

\* Figure 3-13

TABLE 5-VI  
WEIGHT ANALYSIS

<u>Item</u>	<u>Description</u>	<u>Wt/Unit</u>		<u>Est</u>	<u>Qty</u>	<u>Total Wt</u>
		<u>Calc</u>				
I. SOLAR PANEL						
A. Mechanical						
1. Substrate	Aluminum hollowcore, 1.25 hole diam. x 0.004 inch thick skin	0.035 lb/ft <sup>2</sup>			50.0 ft <sup>2</sup>	1.750
2. Beams	Beryllium, 2 in. diam., 0.010 thick	0.05 lb/ft			53.5 ft	2.675
3. Beam fittings	Titanium machinings		0.10		14 ft	1.400
4. Attachment clip	Aluminum extrusion	0.012 lb/ft			56.8 ft	0.682
5. Dielectric film	Kapton H film, 1 mil	0.0072 lb/ft <sup>2</sup>			50.0 ft	0.360
6. Torsion springs	Stainless steel		0.05		4 ft	0.200
						7.067
B. Adhesives (Mech)						
1. H film to substrate	2 mil Narmco 3135	0.0103 lb/ft <sup>2</sup>			9.0 ft	0.093
2. Clip bonding	10 mil Narmco 3135	0.0027 lb/ft			56.8 ft	0.153
3. Beam to fitting	10 mil Narmco 3135	0.005 lb/ft			30 ft	0.150
						0.395
C. Electrical						
1. Solar Cell	10 mil 2 x 2 cm N-P silicon	5.35 x 10 <sup>-4</sup> lb/cell			10,800	5.778
2. Coverglass	Tedlar film	5.0 x 10 <sup>-5</sup> lb/in <sup>2</sup>			8,000	0.400
3. Interconnectors		2.2 x 10 <sup>-5</sup> lb ea.			10,800	0.238
4. Terminals		7.7 x 10 <sup>-4</sup> lb ea.			30	0.023
5. Diodes		0.001 lb ea.			30	0.030
6. Cabling		0.0029 lb/ft			36	0.104
						6.573

TABLE 5-VI (Contd)

## WEIGHT ANALYSIS

<u>Item</u>	<u>Description</u>	<u>Wt./Unit</u>		<u>Qty</u>	<u>Total Wt</u>
		<u>Calc</u>	<u>Est</u>		
D. Adhesives (Elec)					
1. Solar cell	4 mil RTV-41	$1.1 \times 10^{-4}$ lb/cell		10,800	1.188
2. Coverglass	Dow Corning x R63489	$4.4 \times 10^{-5}$ lb/cell		10,800	0.475
					1.663
II. MECHANICAL					
1. Main Boom	Beryllium--60 in. long, 5 in. od x 0.025 thick	0.306 lb/ft		5 ft	1.530
2. Support Brace	Beryllium--71 in. long, 2 in. od x 0.016 thick	0.079 lb/ft		12 ft	0.948
3. Brace fittings	Titanium		0.2	4 ea.	0.800
4. Panel tilt drive	Yoke and worm drive		1.0	1 ea.	1.000
5. Boom rotation drive	Case and worm drive		1.0	1 ea.	1.000
6. Drive motors			0.5	2 ea.	1.000
7. Boom mounting assembly			1.5	1 ea.	1.500
8. Deployment springs			0.25	2 ea.	0.500
9. Latches	Stowed lockup		0.2	3 ea.	0.600
10. Sun sensor			0.1	1 ea.	0.100
11. Electronics	Orientation tracking		1.0	1 ea.	1.000
					9.978
	Subtotal				25.676
	10% allowance for estimate				2.576
	TOTAL WT				28.243
III. ANTENNA					
	Estimate of antenna and drive assembly including arm				3.500

#### 5.5.2 RELIABILITY DEFINITION

The array electrical reliability is defined as the probability that the panel will produce a minimum of 200 watts at noon during the Martian summer season with the panels correctly positioned (perpendicular to the sun vector).

#### 5.5.3 POWER CAPABILITY

The expected power output of the array, under the conditions stated in Subsection 5.5.2, will be 205.7 watts. During the spring-fall season, with the same operating conditions, the power will be 234.4 watts. Since the summer condition permits the least power loss, this environment will be used for the reliability calculations.

#### 5.5.4 FAILURE MODE DISCUSSION

##### 5.5.4.1 Solar Cells

The critical mode for the cell array, in terms of power loss, is the open cell or cells that cause current limiting in the circuit containing the open units.

Shorted cells have less effect on the circuit power loss due to lack of the current limiting effect. As an example, the current loss due to a single open cell in one circuit will reduce the circuit power by approximately 7.5% and the total array output by 0.25% whereas a single shorted cell will reduce the circuit power by a maximum of 1.7% and the overall array output by 0.06%.



#### 5.5.4.2 Diodes

The array will function with shorted diodes under normal operational situations. Parallel redundant diodes will be used in all circuits and each diode is capable of handling the circuit load current. Therefore, the critical mode is the probability of more than one diode opening in a circuit during the mission.

#### 5.5.5 ANALYSIS

##### 5.5.5.1 Method

This design is based on a system using minimal size and weight to produce the required power output. The array is not subject to potential shadowing effects as is the case with the conical solar array and the horizontal axis array discussed in previous reports (EOS 7254-M-5 and 7254-M-6); therefore, the number of circuits required is considerably reduced.

The analysis method used for the shadowed arrays was in terms of section losses, an extremely conservative approach. However, for this array a more detailed analysis, based on individual cell failures, is required because of the small permissible power loss in the system.

The mathematical model utilizes a conservative method of probability calculation by assuming that the array consists of a total of 180 individual cell strings (i.e., 30 circuits x 6 strings per circuit), with each string consisting of 60 cells in series. The loss of a cell is assumed to result in the complete loss of one string.

In order to compare this array with the two previous systems on the same basis (i.e., circuit loss), probability figures have also been calculated for the array using 30 through 34 circuits.

#### 5.5.5.2 Failure Rates

The failure rates are:

$$\begin{aligned}\text{Solar cell} &= 0.01/10^6 \text{ hours} = \lambda_c \\ \text{Diode} &= 0.02/10^6 \text{ hours} = \lambda_d\end{aligned}$$

The cell failure rate is based on the value used for the EOS 770 program for a 2 x 2 cm cell. The diode failure rate is that used for the Surveyor solar panels built by EOS. Operational mission time = 8760 hours.

#### 5.5.5.3 Calculations

##### 5.5.5.3.1 Permissible String Failures

Based on the conditions of Subsection 5.5.2, the string loss is calculated as follows:

$$\begin{aligned}\text{Array power output} &= 205.7 \text{ watts} \\ \text{Allowable power loss} &= 205.7 - 200 = 5.7 \text{ watts} \\ \text{Nominal string power} &= 205.7/180 = 1.14 \text{ watts} \\ \text{Allowable string failures} &= 5.7/1.14 = 5 \text{ strings}\end{aligned}$$

##### 5.5.5.3.2 Diode Reliability

$$\text{Single diode (Rd)} = e^{-\lambda_d t} = e^{-(0.02 \times 8760 \times 10^{-6})}$$

$$R_d = 0.9998$$

$$\text{Redundant diodes (Rdr)} = 1 - (1 - R_d)^2$$

$$R_{dr} = 1 - (1 - 0.9998)^2 = 0.99999$$

#### 5.5.5.3.3 Single String Cell Reliability ( $R_{ss}$ )

$$R_{ss} = e^{-n\lambda t} = e^{-(60 \times 0.01 \times 8760 \times 10^{-6})} = e^{-0.00526}$$

$$R_{ss} = 0.99475$$

#### 5.5.5.3.4 Single String Reliability w/diodes ( $R_s$ )

$$R_s = R_{ss} \times R_{dr} = 0.99475 \times 0.99999$$

$$R_s = 0.99474$$

#### 5.5.5.3.5 Total Array Reliability ( $R_a$ )

The total array reliability is determined by the probability of the loss of five strings and is derived by expanding the first six terms of the binomial distribution.

$$R_a = \sum_{n=0}^6 (p + q)^n = \sum_{n=0}^6 (0.99474 + 0.00526)^{180}$$

$$R_a > 0.998$$

#### 5.5.5.3.6 Calculation Based on Circuit Loss

In order to compare this array reliability with values obtained for the two previous systems on the same basis, calculations based on complete loss of circuits were derived for the array. In addition to the 30 circuit unit, values were also derived for systems containing additional circuits.

These values are summarized as follows:

<u>No. Circuits In Array</u>	<u>Allowable No. of Circuit Failures</u>	<u>Reliability Value - %</u>
30	1	77.31
31	2	93.49
32	3	98.51
33	4	99.71
34	5	99.95

#### 5.5.6 CONCLUSIONS

The vertical axis array has a probability of 99.8% of meeting the minimum power requirements using an analysis based on the allowable number of individual cell failures.

Comparison of the array with the conical array and the horizontal axis array on the same basis (i.e., circuit loss) indicates that the vertical axis array would require an increase to 34 circuits in order to compare favorably with the other systems. It should be noted that calculations based on the loss of circuits result in very conservative reliability values.

SECTION 6

PRELIMINARY MANUFACTURING PLAN

Refer to Section 6 of Volume I

SECTION 7  
PRELIMINARY TEST PLAN

7.1 INTRODUCTION

This section describes the test program proposed for qualifying the JPL/SPA single panel, oriented array for the environments of sterilization, storage and transportation, launch, flight, Mars landing, and one Earth year on the Martian surface. Included are tests of components where they represent substantial innovations and tests to be performed during fabrication to determine acceptability of subassemblies. Additional tests not listed will be performed as required to qualify materials and manufacturing techniques.

We have developed a large body of special techniques for the testing of solar panels, many of which will have direct application to the JPL/SPA program.

7.1.1 DEFINITIONS

- a. Substrate: Any one of four cell-supporting structures which compose the cell array, without cells.
- b. Prototype Panel: Any one of the substrates with "dummy" cells or partial complement of "live" cells. To be used for testing purposes only, not for flight use.
- c. Qualification Panel: Any one of the substrates with "live" cells attached and in final flight configuration. To be used for testing purposes only, not for flight use.
- d. Flight Panel: Any one of the substrates with "live" cells attached and in final flight configuration. To be used for flight use.

- e. Test Module: A group of cells, 6P x 6S, electrically interconnected and mounted to substrate representative of the actual panel substrate but one foot square in size.
- f. Mounting Structure: The support structure and two orientation drive mechanisms, sharing a common main shaft tube. The support structure positions the flight panel and antenna during launch, flight, and landing in a stowed position, and after landing is released and falls away.
- g. Solar Planetary Array or "Array": The complete power system as related to the flight panel and mounting structure.

## 7.2 SOLAR ARRAY TESTS

A summary of the test program is presented in Table 7-I.

TABLE 7-I

### TEST PROGRAM SUMMARY

<u>Table</u>	<u>Item</u>	<u>Qty</u>	<u>Test Description</u>
7-II	Test Module	4	Engineering Evaluation
7-III	Prototype Panel	1	Prototype Panel Test
7-IV	Prototype Array	1	Prototype Panel and Mounting Structure Test
7-V	Qualification Panel	1	Preliminary Flight Acceptance Test
7-VI	Qualification Panel	1	Formal Qualification Test
7-VII	Qualification Array	1	Formal Type Approval Test
7-VIII	Qualification Panel	1	Formal Reliability Test
7-V	Flight Panels	2	Flight Acceptance Test

#### 7.2.1 ENGINEERING EVALUATION TEST

This test shall be performed on 4 test modules consisting of 6P x 6S cells, each mounted on a square foot substrate representative of the flight substrate.

Performance and environmental testing shall be accomplished to establish advance confidence in fabrication techniques, testing, and environmental requirements prior to conducting prototype tests. Performance and environmental test data shall be recorded and maintained. Table 7-II shows the testing sequence for each test.

TABLE 7-II

ENGINEERING EVALUATION TEST SEQUENCE

Item:	Test Module
Quantity:	Four
1.	Mechanical inspection
2.	Simulator test
3.	Application of cover film
4.	Mechanical inspection
5.	Simulator test
6.	Sterilization
7.	Mechanical inspection
8.	Simulator test
9.	Rapid decompression
10.	Mechanical inspection
11.	Simulator test
12.	Mars environment
	7 millibars pressure
	270 mph wind
	1 to 100 $\mu$ abrasive, conductive dust
13.	Mechanical inspection
14.	Simulator test
15.	Accelerated weathering
16.	Mechanical test
17.	Simulator test



### 7.2.2 PROTOTYPE TESTING

This test shall be performed in two parts: first, a prototype panel shall be tested per the testing sequence shown in Table 7-III, and then the panel shall be mounted to a prototype spacecraft and tested for orientation capabilities in a wind tunnel to simulate the dynamic loading conditions per the test sequence shown in Table 7-IV.

TABLE 7-III

#### PROTOTYPE PANEL TEST

Item: Substrate, with dummy cells

Quantity: One

1. Mechanical inspection
2. Vibration (sinusoidal)
3. Mechanical inspection
4. Vibration (random)
5. Mechanical inspection
6. Sterilization
7. Mechanical inspection
8. Rapid decompression
9. Mechanical inspection
10. Temperature cycling
11. Mechanical inspection

TABLE 7-IV

PROTOTYPE PANEL AND MOUNTING STRUCTURE TEST

Item: Prototype array

Quantity: One

1. Mechanical inspection
2. Deployment - horizontal
3. Mechanical inspection
4. Deployment 34° upward
5. Mechanical inspection
6. Deployment 34° downward
7. Mechanical inspection
- 8 through 14. Repeat steps 2 through 7 in an 18.5 mph wind  
(1 atmosphere pressure)
- 15 through 21. Repeat steps 8 through 14 with wind from 90°  
direction

7.2.3 ACCEPTANCE TEST

Acceptance testing will be performed on all flight panels prior to delivery to JPL, and on the qualification panels prior to qualification testing. The electrical and environmental test data shall be recorded and maintained. All sunlight and rooftop tests include diode reverse leakage and insulation resistance tests.

EOS will perform the acceptance tests in the sequence shown in Table 7-V. The acceptance test will be performed on the qualification panel and on each panel of all flight units.

TABLE 7-V

ACCEPTANCE TEST SEQUENCE

To be performed on any flight panel.

1. Sunlight test
2. Acoustic test
3. Mechanical inspection
4. Rooftop test
5. Temperature cycling
6. Mechanical inspection
7. Sunlight test

7.2.4 QUALIFICATION TEST

To be performed on one solar panel.

All individual tests shall be performed without any adjustments and/or repairs being accomplished during such tests. In the event of a test failure, EOS will stop all further testing and shall not proceed before notifying JPL. All data taken during electrical and environmental testing shall be recorded and maintained.

Prior to any qualification testing, the solar panel shall have satisfactorily passed the electrical and environmental requirements of acceptance testing.

Table 7-VI shows the qualification test sequence.

7.2.5 FORMAL TYPE APPROVAL TEST

After completion of the individual qualification panel tests, the unit shall be assembled to a complete mounting structure and a

TABLE 7-VI

## QUALIFICATION TEST SEQUENCE

To be performed on one solar panel.

1. Sunlight test
2. Relative humidity
3. Mechanical inspection
4. Rooftop test
5. Sterilization
6. Mechanical inspection
7. Sunlight test
8. Vibration - transverse axis (sinusoidal and random)
9. Mechanical inspection
10. Vibration - lateral axis (sinusoidal and random)
11. Mechanical inspection
12. Vibration - longitudinal axis (sinusoidal and random)
13. Mechanical inspection
14. Rooftop test
15. Shock  $\pm$  transverse axis
16. Mechanical inspection
17. Shock  $\pm$  lateral axis
18. Mechanical inspection
19. Shock  $\pm$  longitudinal axis
20. Mechanical inspection
21. Rooftop test
22. Acoustic
23. Mechanical inspection
24. Rooftop test
25. Temperature vacuum
26. Mechanical inspection
27. Rooftop test
28. Temperature cycling
29. Mechanical inspection
30. Rooftop test
31. Rapid decompression
32. Mechanical inspection
33. Sunlight test

simulated vehicle body for type approval testing. The testing shall be per the sequence shown in Table 7-VII.

TABLE 7-VII

TYPE APPROVAL TEST

Item:           Qualification Array

- a. Qualification panel
- b. Qualification mounting structure

Quantity: One

1. Mechanical inspection
2. Sunlight test (panel)
3. Vibration - transverse axis (sinusoidal and random)
4. Mechanical inspection
5. Vibration - lateral axis (sinusoidal and random)
6. Mechanical inspection
7. Vibration - vertical axis (sinusoidal and random)
8. Mechanical inspection
9. Rooftop test
10. Shock (general)  $\pm$  transverse axis
11. Mechanical inspection
12. Shock (general)  $\pm$  lateral axis
13. Mechanical inspection
14. Shock (general)  $\pm$  vertical axis
15. Mechanical inspection
16. Rooftop test
17. Type approval system sterilization
18. Mechanical inspection
19. Rooftop test
20. Disassembly
21. Mechanical inspection
22. Sunlight test (panel)

#### 7.2.6 RELIABILITY TEST

EOS will perform the reliability test using the panel previously used during qualification testing.

The panel shall be subjected to a total of 30 days of environmental conditions. Every 120 hours the unit shall be removed from its environment and rooftop tested.

Table 7-VIII shows the test sequence for the reliability tests.

#### NOTE

If wind tunnel test of deployed array shows substantial vibration or oscillation, a reliability test may be required to evaluate this parameter.

TABLE 7-VIII

#### RELIABILITY TEST SEQUENCE

To be performed on one solar panel (used in qualification test sequence, above).

1. Sunlight test
2. Temperature cycle (5 days)
3. Rooftop test
4. Remperature cycle (same as 2)
5. Rooftop test (same as 3)
6. Temperature cycle (same as 2)
7. Rooftop test (same as 3)
8. Temperature cycle (same as 2)
9. Rooftop test (same as 3)
10. Temperature cycle (same as 2)
11. Rooftop test (same as 3)
12. Temperature cycle (same as 2)
13. Sunlight test (same as 1)

### 7.2.7 SHIPPING CONTAINER TEST

The test shall consist of three drops from an elevation of 12 inches. The container shall be dropped once in each plane as follows:

- a. Flat
- b. Edgewise (long edge)
- c. Edgewise (short edge)

The object of these tests is to determine that no physical damage occurs to the SPAs which may be in the container. All data shall be recorded and maintained.

### 7.3 TEST EQUIPMENT AND FIXTURES

EOS has maintained the latest in test equipment to record and resolve data within the parameters of present day requirements.

Three basic means of data acquisition for performance testing of solar devices are employed: digital voltmeters, digital printers, and X-Y recorders. Sun simulators are used to illuminate some of the solar devices; these will be discussed later.

The latest in test equipment is employed for environmental requirements. Digital voltmeters, temperature recorders, and electronic control equipment are a few of those utilized for controlling, resolving, and recording data and/or functions. Presently being used are environmental chambers capable of reaching pressures of  $1 \times 10^{-6}$  torr and simulating space environment conditions of solar panel testing.

Fixtures for vibration and shock, acoustic, temperature cycling, humidity tests, and altitude temperature tests will be specially designed.

#### 7.4 PERFORMANCE TESTING (Sunlight, Rooftop, and Solar Simulator)

EOS will make performance tests for the purpose of acceptance during fabrication levels and final acceptance. The following paragraphs discuss the individual tests in greater detail.

##### 7.4.1 SINGLE CELL TESTING

Individual cell measurements will be made under a tungsten iodine light source, calibrated to an intensity of  $140 \text{ mW/cm}^2$  (AMO). A standard cell, typical in spectral response to cells being fabricated into SPAs, shall be calibrated against a JPL balloon flown standard.

##### 7.4.2 SUBMODULE TESTING

The submodule testing is performed under the same tungsten iodine simulator discussed in Subsection 7.4.1.

The submodules are tested for  $I_{sc}$  (short circuit current) and the current at 485 mV. These tests are performed while the submodule is at a temperature of  $28^\circ \pm 2^\circ\text{C}$ . Calibration of the submodule area (2 cm x 12 cm) will be performed with a standard cell and set for an intensity of  $140 \text{ mW/cm}^2$ . Area uniformity will be held to within  $\pm 1\%$  or less.

The test fixture has the standard 4-point probe electrical contact system, and also employs a vacuum system to aid in securing the submodule to the base.

##### 7.4.3 SAMPLE MODULE TESTING

The 6 x 6 cell sample module used in the test sequence of Table 7-II will be tested under a xenon solar simulator.



#### 7.4.4 PANEL TESTING

EOS will test the SPAs in sunlight. An I-V curve will be produced for each circuit on the panel and for a total panel.

"Sunlight" tests will be performed at Table Mountain, California.

"Rooftop" tests will be performed at the Pasadena facility.

The I-V plots will be drawn with an X-Y recorder and points ( $I_{sc}$  and  $V_{oc}$ ) will be checked against a digital voltmeter. Data acquired during testing (temperature, intensity, panel electrical outputs, date, time, etc.) will be properly recorded and maintained.

Sunlight performance tests are performed when the following conditions exist:

- Sky radiation 10 percent or less
- Sun intensity approximately  $100 \text{ mW/cm}^2$

Data obtained during testing of solar panels is extrapolated from AM1 ( $100 \text{ mW/cm}^2$ ) to AMO ( $140 \text{ mW/cm}^2$ ).

Tests will be performed to determine the characteristic temperature response of the cells and that data will be used to derive panel open circuit voltage.

$I_{sc}$  corrections must be made to correct for sun intensity losses through the Earth's atmosphere. An equation for  $I_{sc}$  correction is as follows:

$$I_{scp_1} = I_{scp_2} \times \frac{I_{scuc}}{I_{scn}}$$

where:  $I_{sc1}$  = the corrected short circuit current for a circuit

$I_{sc2}$  = the recorded short circuit current for a circuit during testing

$I_{scuc}$  = the standard cell, uncollimated, short circuit current reading during testing

$I_{scn}$  = the calibrated AMO short circuit current for the standard cell

Extrapolations for  $I_{sc}$  and  $V_{oc}$  will be determined and a corrected I-V curve shall be replotted for an AMO ( $140 \text{ mW/cm}^2$ ) intensity. The maximum power point will then be determined from this curve.

## SECTION 8

### SUMMARY

This report finalizes the detailed analysis and demonstrates the feasibility of the third of three array concepts of a planetary photovoltaic solar array for operation on the Martian surface.

The system presented here is a single-panel-oriented array meeting all the packaging constraints imposed on the design by JPL in drawing 1002-3236A. The basis of this concept was to present to JPL a system which had orientation capability, and no shadowing restrictions. To accomplish this, it is mandatory that the antenna and solar array be mounted to a common vertical boom elevated above the spacecraft body. This allows the minimum number of circuits (30) to be used to achieve the required power output of 200W under worst case conditions.

Combining the antenna and solar array mounting presents a problem in maintaining the pointing accuracy of the antenna when the system is buffeted by wind gusts. The vertical boom has been sized to minimize the deflection due to wind loads; however, other factors would be present. The drive mechanisms would have to be designed to eliminate, as much as possible, any backlash in the gearing, and the latching mechanism of the vertical boom would have to be of a self-tightening design. Other factors, such as the stability of the spacecraft body and legs and the soil condition where the vehicle landed, would affect the antenna point accuracy, but these are unanswerable at the present time.

The single-panel-oriented array of 30 circuits will meet the desired goal of 20 W/lb at 1 AU, and exceed the minimum power requirement of

200W at solar noon for worst case seasonal conditions. The power outputs for the limiting seasonal conditions are:

Summer Solstice at noon - 205.6W.

Spring/Fall Equinox at noon - 234.4W.

A summary of the system is as follows:

- a. Type of cell - 0.010 in. thick, 2 x 2 cm, N/P, top contact, 1-3 ohm-cm, solderless
- b. Output of cell - 58 mW at 485 mV (AMO)
- c. Number of cells/circuit - 6P x 605 (360)
- d. Number of circuits/array - 30
- e. Number of cells/array - 10,800
- f. Number of orientation drives - 2
- g. Number of orientation drives - 2 for antenna
- h. Orientation mode - continuous motor gear drive, with solar cell sun sensor
- i. Weight summary -
  - (lb)
  - 1. Panel substrates 7.067
  - 2. Adhesives (structural) 0.395
  - 3. Structure and drive 9.978
  - 4. Solar cells and components 6.573
  - 5. Adhesives (cell mtg) 1.663
  - Subtotal 25.676
  - 10% Estimate Allowance 2.567
  - Total 28.243
  - 6. Estimate of antenna and drive 3.500

The power to weight ratio, based on 1 AU, for the output condition of noon at the summer solstice with a solar intensity on the Martian surface of  $46 \text{ mW/cm}^2$  may be found as follows:

Power at Summer Solstice (noon) - 205.6W

Converting to 1 AU by the ratio of:

$$46/140 = 0.328$$

The equivalent array power output at 1 AU is:

$$205.6/0.328 = 626W$$

The specific power at 1 AU would be:

$$626W/28.243 \text{ lb} = 22.2 \text{ W/lb}$$